UNIVERSITY OF MOLISE
Dept. of Medicine and Health Sciences "V. Tiberio"

PhD course in TRANSLATIONAL AND CLINICAL MEDICINE

XXXIV CYCLE

S.S.D Area-05 - Bio 10 Biochemistry

DOCTORAL THESIS

The peculiar processing of LRP8 and its significance for Alzheimer's disease

Tutor:
Prof. Claudio RUSSO

PhD Student:
Emanuele FODERÀ
Matr.164369

Coordinator:
Prof. Giovanni SCAPAGNINI

Academic year: 2020/2021

"How wonderful that we have met with a paradox. Now we have some hope of making progress."

Niels Bohr

INDEX

INTRODUCTION

Dementia: features, figures and types of dementia

Dementia is a syndrome in which there is deterioration in cognitive functions - such as memory, thinking, orientation, comprehension, calculation, learning capacity, language, and judgement – leading to inability to perform normal activities of daily living. According to the Alzheimer's Disease International the number of people with dementia worldwide is estimated at 55 million, and this number is expected to rise to 78 million in 2030 and 139 million in 2050; a new case of dementia occurs somewhere in the world every 3 seconds; the estimated total global societal cost of dementia was US$ 1.3 trillion in 2019, and these costs are expected to surpass US$ 2.8 trillion by 2030. Therefore, dementia has physical, psychological, social and economic impacts, not only for people living with this syndrome, but also for their caregivers, families and society [1].

Dementia is not a single disease, but rather a combination of symptoms and other features that exist together and form a recognized pattern. Several forms of dementia have been described: a) Alzheimer's disease, the most common cause of dementia, characterized by deposition of "plaques" (of amyloid protein) and "neurofibrillary tangles" (of tau protein) in the brain; b) the vascular dementia, the second most common form of dementia, occurs when an arterial disease impairs the blood supply to the brain, which will result in a reduction of neuronal function and eventually the death of brain cells; c) in dementia with Lewy bodies, considered to be the third most common type of dementia, small aggregations of a protein called alpha-synuclein deposit in cells in various areas of the brain, including the cerebral cortex; d) frontotemporal dementia covers a series of conditions that affect the front part of the brain (responsible for planning, emotion, motivation and language);

e) the mixed dementia occurs when more than one type of dementia exists (the most common type is mixed Alzheimer's and vascular dementia, where it is possible observe clinical characteristics and brain changes common to both conditions); f) other conditions can lead to dementia, such as Huntington's disease, corticobasal degeneration, Creutzfeldt-Jacob disease, multiple sclerosis, human immunodeficiency virus-related dementia [2].

Alzheimer's disease: a brief history, hallmarks, symptoms, types of AD and risk factors

Alzheimer's disease (AD) represents the most common neurodegenerative cause of dementia (accounting for an estimated 60% to 80% of cases), with the incidence continuing to grow in part because of the aging world population [3].

The discovery of Alzheimer's disease dates back to 1906, when the clinical psychiatrist and neuroanatomist Alois Alzheimer reported "a peculiar severe disease process of the cerebral cortex" to describe the conditions of his patient Auguste Deter. Five years before, Auguste was taken to Frankfurt Psychiatric Hospital by his husband owing to the worsening of her paranoid symptomatology, sleep disorders, disturbances of memory, aggressiveness, crying, and progressive confusion. The autopsy allowed to Alzheimer to study the morphological and histological characteristics of Auguste's brain and discover the histological alteration that nowadays are considered the hallmarks of AD: the "amyloid plaques" (or "senile plaques") and "neurofibrillary tangles" (NFTs) [4].

In the 1980s was discovered that β-amyloid (Aβ) peptides, a 39-42 residue peptide resulting from the proteolytic processing of Amyloid precursor protein (APP), were the major component of amyloid plaques, whereas tau protein was the major component of the neurofibrillary lesions of AD [5].

Other important features of AD include oxidative stress, mitochondrial dysfunction, inflammation, neuron degeneration [6][7].

Despite amyloid plaques have been considered the main cause of AD for a long time, tau inclusions correlate better with cognitive impairment: in Braak staging, a common method to classify the severity of AD, is the localization of neurofibrillary tangles to define 6 stages of AD: in Stages I and II the NFTs are limited to the transentorhinal region of the brain. Stages III and

IV are when the NFTs are in the limbic regions, which includes the hippocampus. Stages V and VI are when the NFTs are spread in the neocortical regions of the brain [8] .

Although loss of memory is the first symptom of AD, affective and behavioral changes may show: patients with AD display a gradual increase of forgetfulness, decrease attention span, and alterations in mood, often with frustration and agitation. At the end, the patients become dependent on caregivers, unable to walk, incontinent, dysphagic, sometimes with neuromuscular rigidity and other extrapyramidal signs. The death generally occurs for intercurrent diseases such as urinary or respiratory infections, between 3 and 10 years after diagnosis [9][10] [11][12].

The main morphological changes in AD affect the temporal lobe: brain of AD patients show atrophy of hippocampus and entorhinal cortex (which play a pivotal role in memory processing) and amygdala (the integrative center for emotions) [13][14][15].

Based on the onset of symptoms, AD is divided in early onset Alzheimer's disease (EOAD) and late onset Alzheimer's disease (LOAD) if the onset occurs before and after of 65 years of age, respectively.

Based on genetics, instead, it is possible recognize familial AD (FAD) and sporadic AD (SAD).

FAD, the 5% of AD cases, is expressed as a Mendelian trait, with dominant inheritance: it is associated with mutations or overexpression on APP on chromosome 21, mutation on Presenilin 1 (PSEN-1) on chromosome 14 and Presenilin 2 (PSEN-2) on chromosome 1: PSEN-1 and PSEN-2 which represent the catalytic subunits of γ-secretase, the enzyme responsible of APP processing. Mutations in APP, PSEN-1 and PSEN-2 genes are associated with an increment of Aβ peptides, mainly the isoforms 1-42.

On the other hand, SAD represents about the 95% of cases. As opposed to FAD, the etiology of SAD is not well understood and seems to be a combination of genetic and environmental factors.

Apolipoprotein E (ApoE), which binds and carries cholesterol and other lipids into the blood, is deemed to be the main genetic risk factor for AD: in particular the ε4 allele , present in approximately 10-15% of people, lowers the age of onset and increases the risk for LOAD up to three times in heterozygous conditions and twelve times in homozygous subjects [16][17].

APP (Amyloid Precursor protein)

One of the AD hallmarks is represented by amyloid plaques (or senile plaques), extracellular deposits of the amyloid beta (Aβ) protein, especially the highly hydrophobic and aggregation-prone Aβ42. As mentioned before, Aβ derives from the proteolytic processing of Amyloid precursor protein (APP).

APP is a member of a family of conserved type I membrane proteins: three APP homologs, namely APP, APP like protein 1 (APLP1), and 2 (APLP2) have been identified in mammals. These proteins share a conserved structures (including the E1 and E2 domains), with a large extracellular N-terminal domain and a short cytoplasmic C-terminal domain; interestingly, only APP generates the amyloidogenic Aβ peptide.

APP orthologs have been identified in in C. elegans, Drosophila, Zebrafish, and Xenopus Laevis. The human APP gene is located on the long arm of chromosome 21 and contains at least 18 exons. Alternative splicing generates APP mRNAs encoding several isoforms ranging from 365 to 770 amino acid residues (aa). The APP695 isoform is nearly expressed in neurons and accounts for the primary source of APP in brain.

Despite the intense research effort, the physiological role of APP is not well understood: APP could be involved in cell growth, motility, neurite outgrowth, and cell survival, and seems to have a main involvement in neuronal development and repair [18][19].

Full-length APP is sequentially processed by α- (or β-) and γ-secretases. In "Non-amyloidogenic pathway", the first cleavage of APP is performed by alpha-secretase within Aβ domain, precluding the generation of Aβ. APP cleavage by α-secretase produces the C-terminal fragment C83 and sAPPα, the latter with likely neuroprotective properties. The subsequent cleavage of C83 by γ-secretase induces the release of AICD, which forms a ternary complex

(with the adapter protein FE65 and the histone acetyltransferase TIP60) with a yet unclear transcriptional role.

In the "amyloidogenic pathway" APP is firstly cleaved by β-secretase: the neuronal enzyme is mainly an aspartyl-protease, named beta-site APP cleaving enzyme 1 (BACE-1) or memapsin 2. The β-cleavage releases the soluble amyloid protein precursor β (sAPPβ) and a 99-residue C-terminal fragment (called β-CTF or C99). A further BACE-1 cleavage generates a 11-99 fragment (keeping C99 numbering). C-terminal fragments (CTFs) are then processed by γ-secretase, with the liberation of different amyloid intracellular domains (AICDs) and a family of amyloid β-peptides (Aβ): the Aβ oligomerization and fibrillization lead to the senile plaques formation **(Fig. 1)**.

The γ-secretase cleavage on CTFs occurs in three main sites: cleavage at the ε-site forms $A\beta_{49}$ (49 aa), the ζ-site cleavage produces $A\beta_{46}$ and γ -site cleavage $A\beta_{42/40}$ **(Fig. 2)** [20].

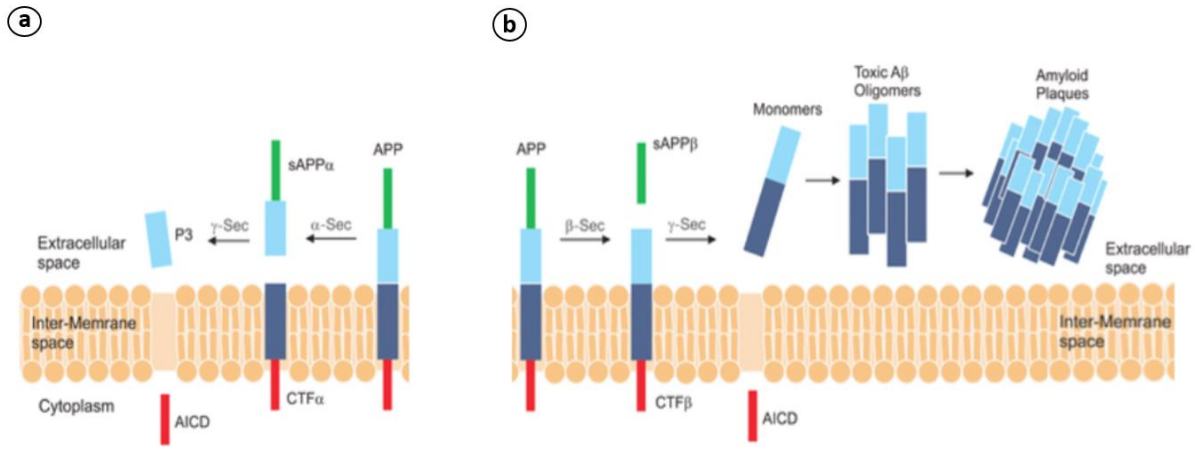

Fig. 1 - Schematic view of (a) Non-amyloidogenic and (b) Amyloidogenic pathways. Adapted from Bachurin et al., 2017.

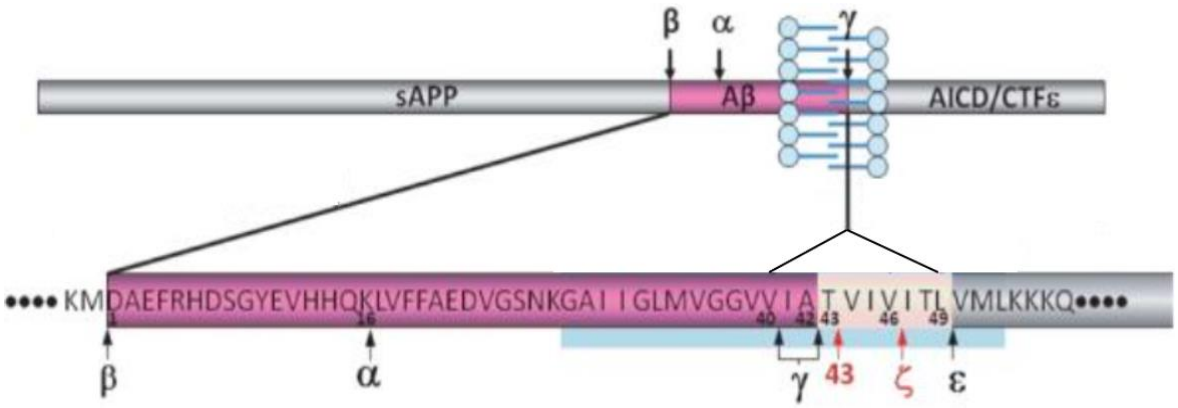

Fig. 2 - Detail of α, β and γ secretases cleavage on APP sequence. (Adapted from Xuemin Xu, 2009)

Alpha secretases reside among members of "a disintegrin and metalloproteinase" (ADAM) family. Several members of ADAM family, such as ADAM-10, ADAM-17 (TACE) and ADAM-9, have been proposed as alpha-secretases. In particular ADAM-10 is regarded as the major physiological alpha-secretase in neurons [21] [22].

The processing of APP is highly complex and a set of proteases could be involved in alternative APP cleavage, with the resulting producing of Aβ peptide variants. In the last years, for example, modified N-terminally truncated Aβ variants, such as Aβ2-42 or AβpE3 (Aβ peptides bearing a pyroglutamate residue in position 3 at the N-terminus), have received a great attention.

Since BACE-1 cannot directly originate these peptides, their production could be induced by the intervention of other proteases.

A candidate directly generating N-terminally truncated Aβ, independent of BACE-1 activity, is the metalloprotease Meprin β. Meprin β is a multi-domain type I transmembrane protein, member of a family of zinc-endopeptidases that is predominantly present as a dimer at the cell surface. N-terminally truncated Aβ2-40 peptides generated by Meprin β dependent on subsequent cleavage of the γ-secretase, but independent of BACE 1, were detected in

supernatants of overexpressing HEK293T cells [23]. Interestingly, increased mRNA levels of Meprin β were measured in AD brain homogenates, supporting a potential role for this enzyme in neurodegeneration.

Different posttranslational modifications of Aβ peptides, which can change the properties of the peptide, have been described: the cyclization of the glutamate residue in position 3 (pGlu3) of Aβ3-40/42, for example, leads to a pyroglutamate-Aβ3-40/42 with a higher aggregation capability. *In vitro* experiments showed that Meprin β cleaves APP at position 3 (p3) with the formation of of Aβ3-40 peptides, containing an N-terminal pyroglumate modification [24].

The amyloid cascade: a controversial hypothesis

The “amyloid cascade hypothesis” proposed by J. Hardy and D.J. Selkoe in 1992 has been for long time the dominant model to explain the AD pathogenesis. It states that the Aβ aggregation triggers a cascade of events ultimately leading to neurofibrillary tangles and cell loss, which are a direct consequence of neurotoxic soluble Aβ peptides [25].

Different evidence led to the amyloid hypothesis: 1) all dominant mutations causing FAD occur or in APP or in Preselins, therefore along the amyloid formation pathway; 2) subjects with Down's syndrome have a duplication of the wild-type APP gene: these subjects exhibit Aβ deposits in the teens, followed by microgliosis, astrocytosis, and neurofibrillary tangles, typical of AD; 3) Apolipoprotein E4, the major risk factor for AD, has been found to impair Aβ clearance from the brain; 4) soluble oligomers of Aβ isolated from AD patients' brains can decrease synapse number, inhibit long-term potentiation, and impairs memory. The human Aβ oligomers also induce hyperphosphorylation and neuritic dystrophy in cultured neurons.

Despite this evidence, a paradox casts a shadow on the robustness of the amyloid cascade hypothesis: the Aβ deposition is not always correlated with neuropathology, while NFTs burden correlates with the clinical phenotype and severity of the disease. For example, not all people with Down’s syndrome, despite the presence of plaques, develop AD. Conversely, neurodegeneration can appear regardless of plaques deposition. Moreover, Aβ deposition occurs in cognitively normal individuals; contrariwise, other markers of advancing AD such as synaptic loss, NFTs, and microglial activation display as the disease progresses. These features are often present in PS conditional KO mice, in absence of plaques. As mentioned above, the mutations causing FAD affect APP and the enzyme processing APP: however FAD represent only the 5% of all AD cases, while the 95% of AD cases are represented by SAD [26].

On the basis of the amyloid hypothesis, in the last 30 years different therapeutic strategies, aimed at clearing Aβ from the brain, have been the object of several clinical trials: these strategies essentially included the use of antibodies vs. Aβ or the use of γ-secretase inhibitors/modulators. Nevertheless, the outcome of the clinical trials based on the amyloid cascade hypothesis were all unsuccessful [27][28]. Finally, it is still lacking the main puzzle piece: the mechanism that from Aβ may lead to tauopathy and neurodegeneration.

Gamma secretase and AD

γ-secretase is a member of the intramembrane-cleaving proteases (I-CliPs) that cleaves type-I transmembrane proteins, such as APP and Notch, through a process named regulated intramembrane proteolysis (RIP). About 150 γ-secretase substrates are now identified.

γ-secretase is a highly hydrophobic complex composed of four integral membrane proteins: Preseniln (PS1; PS2), Nicastrin (Nct); Anterior pharynx defective 1 (APH-1), and presenilin enhancer 2 (PEN-2). PS1 (located on chromosomes 14) and PS2 (located on chromosomes 1) represent the catalytic component of γ -secretase; Nicastrin is a glycoprotein that acts as receptor for γ-secretase substrates, driving them to the active site on presenilin; APH-1 is implicated in γ-secretase positioning and it is required for intramembrane proteolysis of APP [29]; PEN-2 is needed to endoproteolysis of PS into its N- and C-terminal fragments, yielding a catalytically working enzyme **(Fig. 3)** [30].

PS, Nct, APH-1 and PEN-2 are assembled in a tightly controlled manner to form a heterotetrameric complex (with a 1:1:1:1 ratio) with a mass of 174 kDa.

Besides APP, the genetic mutations associated with autosomal dominant familial AD (FAD) affect PSEN-1 (encoding PS1) and PSEN-2 (encoding PS2): mutations within APP gene (many of whom intriguingly situated near γ-secretase cleavage site) account for 10 % of FAD, whereas mutations in PSEN-1 and PSEN-2 genes are linked to 70% and 20 % of the FAD cases, respectively [31].

Presenilin is synthesized as a polypeptide that undergoes endoproteolysis with the formation of a 30 kDa N-terminal fragment (NTF) and a 20 kDa C-terminal fragment (CTF). The biologically active form of PS is represented by the heterodimer deriving from link between the CFT and

NFT moieties, bringing in close proximity two aspartic acids (the two stars in **Fig. 3**) which are essential for the PSENs catalytic activity [32].

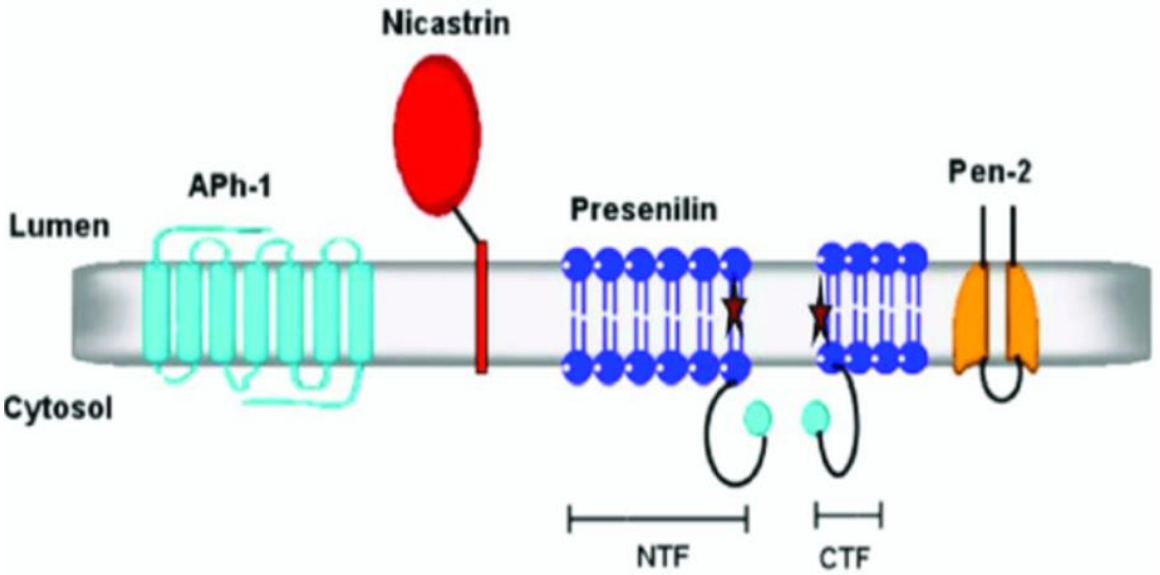

Fig. 3 - Schematic structure of γ-secretase.(Adapted from Narlawar, 2008)

Despite PS1 and PS2 share 65% of sequence identity, they could be involved in different biological processes. To such sense, nearly 200 potentially pathogenic mutations there have been identified in PSEN1, but only 13 pathogenic mutations in PSEN2.

Presenilin FAD mutations were found to alter Aβ production at the level of *γ*-secretase, causing an increment of soluble Aβ42: in particular, familial patients with specific PSEN-1 mutations have also a peculiar brain pattern of soluble Aβ42, characterized by an increased amounts of the more neurotoxic N-terminal truncated and pyroglutamate-modified peptides. The increase of Aβ42 production has been even shown in cell cultures treated with γ-Secretase inhibitors that mimic the effects of pathogenic PS mutations.

Moreover, knockout of PSEN1 dramatically reduced the level of Aβ formation by γ-secretase.

J. Shen and J. Kelleher proposed the “presenilin hypothesis” after their studies in knockout PS mice that showed progressive neurodegeneration with the typical hallmarks of AD, including synaptic loss, neuronal cell death, astrogliosis and tau hyperphosphorylation.

In fact, evidence suggests that loss of essential functions of PS could better explain dementia and neurodegeneration in AD: inactivation of PS in mouse brain causes progressive memory loss and neurodegeneration resembling AD, whereas mouse models with an overproduction of Aβ don’t display neurodegeneration [33][34].

The fact that loss of PS function in mouse brain mimics the conditions observed in AD raised the possibility that FAD-linked mutations in PS may be likely related to a "loss-of-function" of γ-secretase [35].

Other hypothesis explaining AD

Since amyloid accumulation is not always correlated to dementia or neurodegeneration, other hypothesis have been taken into account aside from the amyloid cascade hypothesis [36]. Below some of the most credited alternative hypothesis to explain the AD pathogenesis will be described.

Tau hypothesis

As mentioned before, AD is characterized by two major pathological lesions in the brain: amyloid plaques and neurofibrillary tangles (NFTs), the latter composed of hyperphosphorylated tau.

The tau hypothesis states that AD is caused by NFTs deriving from excessive or abnormal phosphorylation of tau protein [37]. GSK-3β represents the major suspected for the hyperphosphorylation of tau: GSK-3β inhibition with lithium was associated with a significant decrease in CSF concentrations [38].

Tau, encoded by MAPT gene (situated on chromosome 17), is a microtubule associated protein (MAP); it is hydrophilic, highly soluble and expressed mainly in neurons.

Tau protein consists of four primary domains: the N-terminal domain, the proline-rich domain, the microtubule-binding domain, and the C-terminal region (**Fig. 4**).

Alternative splicing of the N-terminal and microtubule-binding domains yields six isoforms in the CNS. The microtubule-binding domain includes R1, R2, R3 and R4 domains: Repeat domains R1, R3 and R4 are constitutive, while only the 4-repeat isoform includes R2 domain. The 3-repeat (3R) and 4-repeat (4R) isoforms are maintained in a balanced ratio (1:1) and a disruption of 3R and 4R ratio has been implicated in AD as well as other tauopathies.

Although the main function of tau is to promote microtubule assembly and stability, tau-knockout mouse model does not impair microtubule assembly or axonal transport and does not show severe phenotype, suggesting that the normal functions of tau might be compensated by various microtubule associated proteins.

Tau has been suggested to be involved in affecting synaptic function and maintaining neuronal projections due to its role in axonal microtubule assembly; thus, the loss of tau function in microtubule binding may lead to a tau aggregation with a consequent synaptic dysfunction and neurodegeneration, resulting in a memory deficit in AD. The molecular mechanism is unknown but it likely involves regulation of NMDA or AMPA receptors [39].

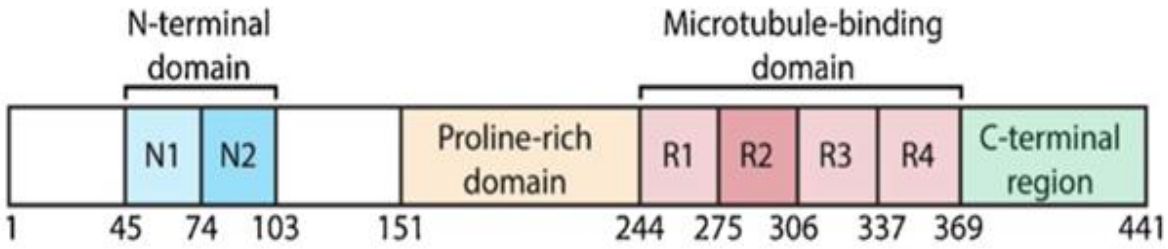

Fig. 4 – Schematic organization of tau protein domains (Adapted from Naseri et al., 2019)

Inflammation hypothesis

Cells activating inflammation in central nervous system (CNS) could have a role in early stages of AD: reactive gliosis and neuroinflammation are indeed hallmarks of AD.

Microglia are cells of the innate immune system and represent the macrophages of the CNS. It is widely accepted that microglial-mediated inflammation contributes to the progression of Alzheimer's disease [40]. In presence of senile plaques, reactive microglia and astrocytes surround amyloid plaques and secrete numerous pro-inflammatory cytokines [41].

Tau protein can be phagocytosed by microglia and activated microglia are frequently found in the closeness of NFTs in the hippocampus of AD patients: these evidence represent an indication of a close relationship between the inflammatory response and tau neurofibrillary lesions [42].

Cell cycle hypothesis

Neurons typically remain in G0, a nondividing, nonreplicating phase of the cell cycle. However, neurons can exit from G0 phase if subject to loss of synaptic connections, chronic exposure to oxidative stress or stress hormones (like glucocorticoids) and reenter into a cell cycle that leads to cell death through apoptosis. The aberrant re-expression of many cell cycle-related proteins and an inappropriate cell cycle control have been noted in vulnerable neuronal populations. The cell cycle hypothesis also attempts to explain the typical hallmarks observed in AD. The intracellular accumulation of highly phosphorylated tau, for example, is linked to the cell cycle: in fact, in addition to regulating the cell cycle, cyclin-dependent kinases (CDKs) are implicated in tau phosphorylation. Moreover, CDKs expression precedes the emergence of hyperphosphorylated tau, suggesting a cause-effect connection [43].

Cholinergic and ROS hypothesis

Acetylcholine (ACh) is an important neurotransmitter released by cholinergic neurons, with a crucial role in physiological processes, such as attention, learning and memory.

The cholinergic hypothesis states that there is a relationship between the cholinergic neurons damage and the pathological changes correlated with cognitive impairment in AD. Based on this consideration, cholinesterase inhibitors were used in AD treatment. Tacrine was the first cholinesterase inhibitor approved for the treatment of Alzheimer's disease, but it was withdrawn due to severe side effects. To date, the cholinesterase inhibition turned out to be just a symptomatic relief treatment with marginal benefits.

Our brain uses the 20% of the body's oxygen: that means that brain undergoes ROS exposure because of mitochondrial respiration. In fact, AD is highly associated with cellular oxidative stress, protein oxidation and nitration, lipid peroxidation and, since Aβ can also induce ROS production, the accumulation of Aβ is correlated to oxidative stress. For this reason, the treatment with antioxidant compounds should provide protection against oxidative stress and Aβ toxicity in theory. Nevertheless, antioxidant strategy showed low potency to stop the progression of AD and thus it is proposed to be part of a combination therapy [36].

Apolipoprotein E (APOE)

ApoE gene is located on chromosome 19 and encodes a glycoprotein that is 299 amino acids long. It is synthesized in various tissues: in the CNS, APOE is mainly expressed in astrocytes and microglia. APOE plays a critical role in redistributing cholesterol and other lipids to neurons, and this process is crucial for the maintenance of synaptic integrity and plasticity. ApoE exerts its function on neurons through the LDL receptor (LDLR) family members, which are major APOE receptors and involved in APOE-mediated lipid metabolism.

Variation in 2 single nucleotide polymorphisms (SNPs) within the *APOE* gene gives rise 3 different isoforms (ε2, ε3, and ε4), which are differentiated on the basis of cysteine and arginine residue interchanges at positions 112 and 158 in the amino acid sequence.

ApoE allele frequencies show different values on the basis of the geographical regions, with ranges of 6.7%–10.0% (APOE ε2), 75.3%–82.8% (APOE ε3), and 7.5%–15.6% (APOE ε4) [44].

ApoE represents the strongest genetic risk factor for Alzheimer's disease: in particular, the presence of ε4 allele is associated with an increased risk of AD, whereas ε2 is associated with a decreased risk of AD in comparison with the common ε3 allele. APOE ε4 is associated both an early onset and a greater severity of AD, likely playing a role in Aβ deposition, tau tangle formation, neuroinflammation and other features of AD.

APOE ε4 heterozygous increases the risk of AD onset 3–4-fold, while ε4 homozygous increases the risk 9–15-fold [45] .

In vitro and *in vivo* data suggest that ApoE interacts with Aβ and plays a role in Aβ removal; thus, the disfunction of ApoE in Aβ clearance is thought to be critical in brain plaque deposition: subjects with AD carrying the ApoE ε4 isoform have a greater number of Aβ plaques in comparison with ApoE ε3 carriers [46]. However, it is also possible that the role of

ApoE ε4 may be linked to its activity as main cholesterol carrier in brain and to its role as signalling molecule through its receptors bearing to the LDL receptor family.

Lipoprotein Receptor-related Protein 8 (LRP8): a crossroad between APP, Gamma Secretase and ApoE

The low-density lipoprotein receptor (LDLR) family is composed of structurally related single transmembrane receptors.

These receptors mediate the signalling and/or trafficking of extracellular ligands, such as apolipoprotein E (apoE), which is crucial for the uptake and redistribution of lipids and cholesterol, the latter being an essential component of membrane and required for the correct function of synapses.

Since the APOE ε4 allele is strictly related to the risk for late-onset Alzheimer's disease, the role of LDLR family in AD pathogenesis has been widely evaluated: LRP1, for example, modulates Aβ endocytic pathways and clearance [47], whereas Lipoprotein Receptor-related Protein 8 (LRP8), also known as Apolipoprotein E Receptor 2 (ApoER2) is involved in learning and memory processing.

For instance, APOE ε4 allele has been associated to impairment of Aβ recycling, impairment of NMDA receptor phosphorylation by Reelin (a pivotal event for synaptic plasticity) and reduction of neuronal surface expression of LRP8/Apoer2, which is known to interact and affect the APP processing [48].

LRP8 is expressed by neurons throughout the brain [45]; it represents the main receptor for ApoE, pivotal in cholesterol homeostasis, and for Reelin, a large secreted extracellular matrix glycoprotein whose signal is crucial for neuronal migration and development and, in adult brain, for synaptic plasticity and neuronal signalling [49].

As a result of the bound with Reelin, ApoER2 clusters and induces the phosphorylation of Reelin-disabled 1 (Dab1), a cytoplasmatic adaptor highly expressed in neurons [50]. Dab1 is

one of several adaptors (including Fe65, X11α, JIP1) binding the NPXY motif in C-terminus of APP as well as LRP8: on one hand, NPXY motif is implicated in endocytosis of APP and LRP8; on the other hand, promoting the interaction with other proteins, could mediate signal transduction pathways of these receptors [51][52].

Moreover, the interaction of Dab1 with NPXY motif of LRP8 initiates a kinase cascade starting with Src kinases activation, then phosphoinositide-3-kinase (PI3K), which subsequently activates protein kinase B (also known as Akt), ending with the phosphorylation and inhibition of GSK-3β, the major kinase that phosphorylates tau protein [53].

Reeler is a mouse mutant (with an autosomal and recessive mutation) lacking of a functional Reelin. This mouse, which represents an attractive model to study neuronal migration, exhibits severe cytoarchitectonic malformations due to the uncontrolled neuronal migration into the neocortex [54].

Interestingly, Dab1-deficient mice (identified as a naturally occurring strain called *scrambler* and also generated by gene knockout), ApoER2 double-knockout mutants and APP conditional knockout mouse line develop a phenotype indistinguishable from Reeler [55][56][57].

Reelin, which is essential for the correct positioning of neurons and the lamination of the cortex and the cerebellum, also enhances long-term potentiation (LTP) in the adult hippocampus, modulating synaptic plasticity and learning in the adult mouse brain. In CNS synaptic plasticity and synaptic strength are controlled by NMDA receptors, ionotropic glutamate receptors that, through Ca^{2+} entry into the neurons, regulate the synapse formation during development and synaptic plasticity and LTP in the adult brain.

It has been shown that, in mouse neurons, Reelin increases Ca^{2+} entry through NMDA receptors and that the interaction of Reelin with LRP8 and Dab1 phosphorylation are essential for this event: Dab1 knockout neurons, or cells in which the interaction of Reelin with LRP8 is blocked by a receptor antagonist (RAP), abolish this modulatory activity of Reelin.

Thus ApoER2, mediating the Reelin pathway, may affect learning and memory by modulating NMDA receptor functions [58]. In this regard, LRP8-KO mice show a severe impairment in freezing behaviors that reflects a loss of long-term memory formation [59].

The interaction among ApoER2, NMDA receptor and PSD-95 (a postsynaptic scaffolding protein in excitatory neurons), demonstrated in mouse neurons, leads to an increase of surface levels and cleavage of LRP8; the intramembranous cleavages of LRP8 is also promoted by APOE, which affects the metabolism of LRP8 C-terminal fragments (LICDs) [60].

To such sense, the cleavage of apoE receptors could be important for the release of their intracellular domain, which could move from the membrane to the nucleus. In particular, *in vivo* experiments in KO-LRP8 mice showed that LRP8 undergoes Reelin-induced γ-secretase-dependent cleavage with the release of 14 kDa intracellular domain (ICD), which translocates into the nucleus and shows a transactivation activity in a GAL4-based transactivation assays. Conversely, the block of γ-secretase activity apparently leads to abolish the Reelin-induced transcriptional changes, suggesting that γ-secretase cleavage on LRP8 is crucial for the Reelin-induced synapse-to-nucleus communication [59].

Therefore, LRP8 intracellular domain is considered critical for the modulation of Reelin activity: in particular, Reelin enhances LTP through a mechanism that requires the presence of amino acids encoded by exon 18 in human (exon 19 in mouse) in the intracellular domain of Apoer2. This exon encodes a proline-rich region composed of 59 aa required for Reelin-

induced tyrosine phosphorylation of NMDA receptor subunits. For this reason the C-terminus of LRP8 is considered pivotal for learning and memory [61].

It has been established that LRP8 negatively affects APP internalization, increasing the cell surface APP levels and, in turn, Aβ production; for this function, the integrity of NPXY motif of LRP8 is required [62].

Similarly, it has been hypothesized that the impairment of Aβ-induced reelin activity goes through the Reelin receptor: in fact, Aβ has been demonstrated to decrease the LRP8 C-terminal fragments and increase the levels of Reelin in AD patients, suggesting a modulatory role on Reelin expression of C-terminus of LRP8 [63].

Other cytoplasmatic adaptors that bind APP, besides Dab1, can bind LRP8. Very interesting is the link between AICD (APP intracellular domain, released after γ-secretase cleavage on APP) with FE65 adaptor and the histone acetyltransferase HTATIP (TIP60/KAT5), with the formation of a ternary complex which it is thought to have a transcriptional function: among the genes that it could regulate there is also GSK3β [64].

FE65 adaptor binds also the NPXY motif of LRP8, forming a complex with both APP and LRP8 receptors and affecting their processing [65].

Besides the intracellular interaction, the extracellular interaction between APP and LRP8 has been demonstrated by coimmunoprecipitation experiments on primary neurons. For this interaction, F-spondin, a protein secreted by cells of the floor plate and regulating the neuronal outgrowth, is crucial. It has been proven that F-spondin interacts with the extracellular domain of both APP and LRP8 in primary neurons and affects the processing of

both receptors: in particular, the bound of F-spondin decreases the β-cleavage of APP and increases the levels of α-CTF of APP and CTF of ApoER2.

Interestingly, the use of receptor-associated protein (RAP), an inhibitor of the apoE receptor family leads to a block of APP β-CTF reduction, suggesting the participation of ApoER2 in APP processing [63].

AIM OF THE STUDY

In this scenario we considered that the “amyloid only hypothesis” should be overcome. We believe that LRP8 is a central receptor for the development of AD since: 1) it interacts with APP (regulating some functions such as amyloid formation); 2) it is the receptor of ApoE, pivotal for the transport of cholesterol, and main risk factor for AD; 3) it is processed by gamma secretase, linking all the genetic components of the disease. Moreover, LRP8 has a fundamental role in neuronal homeostasis as it regulates both metabolic aspects (selenium and cholesterol turnover) and signalling: NMDA coupling, neuronal migration (as reelin receptor), dendritic arborization. Finally, LRP8, like APP, has a transcriptional activity at neuronal level, mediated by its processing, which is however poorly described. In our lab we focused our experiments on multiple aspects of LRP8 processing, interactions and localization. Our results indicate essentially that the processing of LRP8 is conditioned by APP and also by APP’s C-terminal fragments. From the literature in known that LRP8 modulates Aβ formation, however we have also evidence that APP and C99, when overexpressed, enhance LICDs. Studying the effect of ApoE over LRP8, we have data showing a clear role of ApoE, through LRP8, in sorting into extracellular vesicles (exosomes) both APP’s derived CTFs and LICDs from LRP8. Finally, we have evidence that the inhibition of γ-secretase enhances the level of LICDs. Few information is available regarding the transcriptional role of LRP8, its nuclear localization, which are its targets and whether these features could depend by APP or by γ-secretase. For these reasons we here explore the processing of LRP8 and its putative nuclear signalling and transcriptional activity, trying to understand its role in neurodegeneration.

MATERIALS AND METHODS

Human Brain Samples

Human frontal cortices were obtained by autopsy from clinically and neuropathologically verified (CERAD criteria) cases of sporadic late onset AD (SAD: total n. 19, average age 77,63 ± 12,47 years-old; FAD: total n. 9 with mutation on PSEN1 or PSEN2, average age 45,78 ± 5,56 years-old) and age-matched healthy control cases (total n. 16, average age 78,00 ± 10,16 years-old), in which AD has been excluded by clinical, autopsy examination and immunohistochemical analysis, as described in **Table 1.**

Table 1. *Demographic and clinical data of the patients analyzed*

ID	Sex	Age (y.o.)	ApoE genotype	Neuropa-thological diagnosis	Braak Staging	PSEN1/ PSEN2 Mutation	Post-mortem interval (h)	Brain weight (g)	Notes
A94-122	N.A.	82	3,4	Control	-	-	-	-	-
497	F	49	3,3	Control	I	-	11:38	-	-
673	F	80	3,3	Control	I	-	01:09	-	AS: mild
787	F	90	3,3	Control	I	-	10:37	-	AS: mild
984	F	65	3,3	DC	I	-	13:34	-	-
1037	F	88	2,3	Control	I	-	20:30	-	AA: mild
963	F	82	3,3	Control	III	-	08:07	-	AA: severe
3482	F	79	-	Control	-	-	14:00	1060	-
542	M	82	3,3	Control	I	-	03:15	-	AS: mild
1169	M	88	2,3	Control	-	-	17:20	-	-
3298	M	79	N.A.	Control	-	-	22:00	1320	-
3484	M	72	3,4	Control	-	-	12:12	1380	-
4294	M	80	3,3	Control	-	-	19:12	1270	-
4307	M	84	3,4	Control	-	-	11:48	1250	-
4308	M	70	3,3	Control	-	-	11:48	1090	-
591	F	78	3,3	Control	I	-	05:31	-	-
86	M	84	3,4	SAD	V	-	00:40	-	AS: moderate
648	F	81	3,4	SAD	V	-	02:15	-	0
863	M	83	3,3	SAD	V	-	02:00	-	AS: severe
901	F	80	4,4	SAD	V	-	02:30	-	AS: moderate, AA: moderate
942	F	88	3,4	SAD	V	-	09:34	-	AS: severe
960	F	88	4,4	SAD	V	-	13:49	-	AS: moderate, AA: moderate
977	M	80	4,4	SAD	V	-	06:30	-	AA: mild
990	F	80	3,3	SAD	V	-	05:09	-	AS. mild
1142	F	87	3,4	SAD	V	-	13:00	-	AA: mild
3233	F	78	3,3	SAD	N.A.	-	12:18	850	-
3268	F	89	2,3	SAD	N.A.	-	18:24	1000	-
3278	F	81	3,4	SAD	N.A.	-	11:18	1100	-
3285	F	61	3,4	SAD	N.A.	-	07:30	940	-
3288	F	41	2,3	SAD	N.A.	-	23:00	940	-
3291	F	55	N.A.	SAD	N.A.	-	13:15	960	-
3301	F	80	3,4	SAD	N.A.	-	13:45	990	-
3316	F	77	3,3	SAD	V	-	13:00	900	-
3327	M	88	3,4	SAD	IV	-	09:45	940	-
3329	F	74	3,3	SAD	VI	-	14:00	1220	-
00/371°5	M	50	3,3	FAD	V	PSEN2 M239I	N.A.	N.A.	-
00/371°6	M	45	3,3	FAD	N.A.	PSEN2 M239I	N.A.	N.A.	
1024	F	58	3,3	FAD	V	PSEN1 H163R	26:07:00	-	MCKeith DLB limbic
124	M	40	3,3	FAD	V	PSEN1 M146L	04:30	-	-
178	M	44	3,3	FAD	V	PSEN1 H163R	22:09	-	-
313	F	48	3,4	FAD	IV	PSEN1 H163R	16:00	-	-
734	M	41	2,3	FAD	V	PSEN1 M139I	11:30	-	AA: moderate
773	M	43	3,3	FAD	IV	PSEN1 M139I	13:00	-	-
967	F	43	3,4	FAD	VI	PSEN1 M139I	05:00	-	-

M: male; F: female; DC: disease control; CERAD: Consortium to Establish a Registry for Alzheimer's Disease; AS: amyloid staging; AA: amyloid angiopathy; MCKeith DLB limbic: Dementia with limbic Lewy bodies; N.A.: not available.

Cell cultures

Neuro 2A (N2A) cells (a mouse neuroblastoma immortalized cell line) , stably transfected with the plasmid encoding for LRP8-ddk-myc tag were grown in t75 Cell Culture Flasks in DMEM (Dulbecco's Minimum Eagle Medium) supplemented with 10% Fetal Bovine Serum (FBS) decomplemented at 56°C for 30 minutes, 1% L-glutamine (2 mM in 0.85% NaCl), 1% penicillin (50 U/L) and streptomycin (50 µg/mL) in a humidified atmosphere at 37°C with 5% CO2: all these products were purchased from Gibco, USA. N2A LRP8-ddk-myc cells were cultured with additional Geneticin (G418 Sigma, USA), a selection antibiotic that allow the selection of cells that express the plasmid LRP8-ddk-myc.

DAPT treatment

Neuro 2A (N2A) cells, stably transfected with human LRP8 bearing a C-terminal ddk-myc tag (LRP8-ddk-myc), were cultured in flask t75 until to ~70% of confluence, as described in the previous section. Subsequent, cells were starved with DMEM deprived from serum and treated for 16h (overnight, O/N) either with vehicle (DMSO) or with the γ-secretase inhibitor DAPT 10 µM (Tocris Bioscience (UK). Cells were then lysed in RIPA Buffer 1x, centrifuged at 14000 rpm for 15 minutes at 4^{o} C and supernatants collected in a fresh tube and or used for the protein quantification or stored at -20°C.

Actinonin treatment

Neuro 2A (N2A) cells, stably transfected with human LRP8 bearing a C-terminal ddk-myc tag (LRP8-ddk-myc), were cultured in flask t75 until to ~70% of confluence, as described in "Cell cultures" section. Subsequent, cells were starved with DMEM deprived from serum and treated for 16h with Actinonin (Sigma-Adrich- USA) 50, 100, 200 µM .

Controls are vehicle-treated cells with ethanol. Cells were then lysed in RIPA Buffer 1x, centrifuged at 14000 rpm for 15 minutes at 4o C and, supernatants collected in a fresh tube and or used for the protein quantification or stored at -20°C.

Nuclear extraction from N2A cells

Nuclear extraction was performed on N2A cells, stably transfected with human LRP8 bearing a C-terminal ddk-myc tag (LRP8-ddk-myc), by using the "Qproteome Cell Compartment Kit" (Qiagen, Germany).

The kit, optimized for 5 x 10^6 cells, contains:

1. *Lysis Buffer*, which, disrupting the plasma membrane without solubilizing it, allows to recover the cytosol proteins.
2. *Extraction Buffer CE2*, which enables the extraction of the plasma membrane proteins.
3. *Extraction Buffer CE3*, for membrane-bound nuclear proteins recovery.
4. *Benzonase® Nuclease*, for the release of proteins bound to the nucleic acids (such as histones).
5. *Buffer CE4*, which is useful to extract the cytoskeletal proteins.
6. *Protease Inhibitor Solution (100 x)*, needed to be added in Lysis, CE1, CE2 and CE3 Buffers.

The nuclear extraction was performed as follows:

a. cells were cultured on t75 flasks to ~70% of confluence and treated with Actinonin or DAPT for 16 h in a serum-free medium;
b. cell culture medium was removed, and cultured cells were collected in 2 mL of ice-cold PBS 1x, centrifuged at 500 x g for 10 minutes at 4° C, the supernatant removed and discarded;
c. for 2 times, the pellet was resuspended in ice-cold PBS 1x and centrifuged at 500 x g for 10 minutes at 4° C, discarding the supernatant;
d. the pellet was resuspended in ice-cold *Lysis Buffer* containing Protease Inhibitor Solution 1x; incubated for 10 minutes at 4° C on end-over-end shaker and centrifuged at 1000 x g for 10 minutes at 4° C;
e. the supernatant, containing the cytosol proteins, was transferred in a fresh microcentrifuge tube;
f. the pellet was resuspended in ice-cold *Extraction Buffer CE2* containing Protease Inhibitor Solution 1x, incubated for 30 minutes at 4° C on end-over-end shaker and centrifuged at 6000 x g for 10 minutes at 4oC;
g. the supernatant, containing the membrane proteins, was transferred in a fresh microcentrifuge tube;
h. the pellet was resuspended *in Benzonase® Nuclease*, incubated 15 minutes at room temperature, added Extraction Buffer CE3 containing Protease Inhibitor Solution 1x, incubated for 10 minutes at 4° C on end-over-end shaker and centrifuged at 6800 x g for 10 minutes at 4° C;

i. the supernatant, containing the nuclear proteins was transferred in a fresh tube, while the pellet was resuspended in *Extraction Buffer CE4* (without Protease Inhibitor Solution);

j. 5 volumes of cold methanol anhydrous were then added into the tube containing the nuclear proteins and left at -20° C for 16 hours. Subsequently, the solution was centrifuged at 4000 rpm for 15 minutes at 4° C; discarded the supernatant, let the pellet to dry and resuspended it in dH_2O.

The proteins of all the fractions were measured by using Bradford (Bio-Rad, Italy) and BSA (Merck-Millipore, USA) curve for SDS-PAGE and Western Blots analysis.

Immunohistochemistry and Immunocytochemistry experiments

Immunohistochemistry (IHC) on human cerebral cortex was done on 6-7 µm paraffin-embedded brain slices from SAD, FAD and control subjects, reported in the **Table 1.** Sections were de-waxed in xylene and rehydrated through graded alcohols. Slides were heated in a microwave in 10 mM sodium citrate buffer (pH 6.0) for epitope retrieval, incubated with PBS 1x + 0.3% Triton for 10 minutes, saturated with 10% normal goat serum (NGS) in PBS 1x and incubated O/N at 4°C with a 1:100 dilution of primary antibodies in PBS 1x and 1% NGS. After repeated washes in PBS, the sections were incubated with Alexa-488 or -568-conjugated secondary antibodies and DAPI for nuclear staining for 45 min in PBS 1x, washed again and further incubated for 10 minutes with a fresh solution of 0,3% Sudan Black (Applichem, USA) in 70% ethanol to reduce spontaneous autofluorescence. After washing PBS 1x, slides were

finally mounted with Mowiol. Negative controls were performed omitting the primary antibodies and using non-specific IgGs.

In order to quantify the fluorescence intensity of the images, we fine-tuned an “intensity profile” based-analysis, consisting in measuring values along 550 µm-vector designed from deeper cortical layers to molecular layer I. We analysed 10 vectors for each cortical area investigated, considering a total of 2 different areas for each AD and control case. To study the overall signal of LRP8 antibody in the image, we evaluated the area under the curve of the intensity profile and analyzed the data by using the One-Way ANOVA followed by Dunnett’s post hoc test.

Immunocytochemistry (ICC) experiments:

1. cells were cultured on 12 mm round glass slips until at ~70% of confluence and, after that, treated with Actinonin or DAPT for 16 h in a serum-free medium;
2. cell culture medium was removed and cultured cells were fixed with cold 4% paraformaldehyde for 15 minutes;
3. cell cultures were washed 3 times with PBS 1x for 3 minutes, treated 2 times with PBS 1x + 0,1 M glycine (Sigma, USA) for 5 minutes and again 3 times washed with PBS 1x for 3 minutes;
4. cell cultures were incubated with Blocking solution (PBS 1x + 10% NGS, Sigma, USA) for 20 minutes, then with primary antibody for 45 minutes (rabbit polyclonal anti-LRP8, named GS1, GeneScript, USA) and washed with PBS 1x 3 times for 3 minutes and then 1 time for 5 minutes;

5. cell cultures were incubated with a solution (PBS 1x + 10% NGS) with secondary antibody (anti-rabbit red Alexa Fluor® 568, ThermoFisher, USA) and DAPI (Sigma, USA); and then washed with PBS 1x 3 times for 3 minutes and then 1 time for 5 minutes;
6. finally, cell cultures were cover slipped using Mowiol (Sigma, USA) as mounting solution over night at room temperature.

All IHC and ICC images were visualized and acquired with the C2/C2si Confocal microscope (Nikon, Japan), mounted on a Ti2-U basis with a Nikon 60X1.4 Plan Apo objective, by using a DS-Qi2 camera (Nikon, Japan); the images then were analyzed with the NIS-Elements software (Nikon, Japan).

SDS-PAGE and Western Blot experiments

SDS-PAGE and Western Blot experiments were performed on:

1. Brain samples, homogenized with RIPA Buffer 1x in a ratio 1:4. RIPA Buffer 1x contains 500 mM Tris pH 7.6, 50 mM EDTA, 5% sodium deoxycholate, 1% SDS, 10% NP40, complemented with protease inhibitors 1x, sodium orthovanadate 1 mM (Na_3VO_4), sodium fluoride 10 mM (NaF) and phenylmethanesulfonyl fluoride 1 mM (PMSF). The homogenization occurred by using a rotor-stator homogenizer at maximum speed for 30 seconds, then were centrifuged at 20,000 x g for 20 minutes at 4°C and supernatants were collected, as described in literature [9].

2. Cell cultures, washed three times with Phosphate-Buffered Saline (PBS) 1x and lysed with RIPA Buffer 1x. The samples were collected with scrapers and incubated for 20 minutes in ice, then centrifuged at 14,000 x g for 15 minutes and supernatants were collected.

3. Nuclear and cytosol proteins deriving from the extraction with "Qproteome Cell Compartment Kit" (see the paragrath "Nuclear extraction from N2A cells" in "MATERIALS AND METHODS" part).

Samples protein amount was determined by using Bradford (Bio-Rad, Italy) and BSA curve. The samples were then loaded with Sample Buffer 2x (SDS 8%, glycerol 24%, Tris 100 mM, tricine 100 mM, dithiothreitol 15 mg, Coomassie brilliant blue g-250 0.05%) in a Tris-Tricine SDS PolyAcrylamide Gel Electrophoresis (SDS–PAGE), with 10 and 12,5% and transferred to a PVDF membrane 0.22 µm (Amersham, UK). Membranes were blocked by an incubation of 2 h

in Phosphate-buffered saline Tween-20 (PBS-T) containing 5% non-fat dried milk and blotted over night with the primary antibodies: rabbit polyclonal anti-LRP8 (named GS1, GeneScript, USA), rabbit polyclonal anti- C-terminus of APP (Zymed, Zymed Laboratories, USA), mouse monoclonal anti- β-tubulin (D-10 sc-5274), Histone H3 (1G1 sc-517576, Santa Cruz, USA) and Lamin B1 (B-10 sc-374015, Santa Cruz, USA). After washing with PBS-T, the membranes were incubated for 1 h at room temperature with the peroxidase-conjugated secondary antibodies, mouse or rabbit according to the experimental needs. After washing the reactive bands were revealed with ECL-Plus Western Blotting Detection Reagents (GE Healthcare Life Sciences, United Kingdom).

Images were acquired by using the automated gel imaging instrument Gel Doc EZ System (Bio-Rad, Italy) and the Alliance™Q9 Atom Advanced-Auto (Uvitec Ltd, United Kingdom). Densitometric analysis of protein bands was performed by using ImageLab software (Bio-Rad, Italy) and NineAlliance sofware (Uvitec Ltd, United Kingdom) normalizing the data to β-tubulin, Histone H3 and Lamin B1.

Quantitative PCR (Real Time PCR, RT-PCR)

Unlike the PCR technique, Real Time PCR allows the quantitative characterization of the transcript, monitoring the quantity of template DNA during the exponential phase of the amplification curve (before the plateau). RT-PCR was conducted using Taqman assays (Applied Biosystems, USA). The TaqMan probes are designed to increase the specificity of quantitative PCR. TaqMan probes consist of a fluorophore covalently attached to the 5'-end and a quencher at the 3'-end. Relying on the 5´–3´ exonuclease activity of Taq polymerase to cleave the probe during the "annealing" phase of PCR, the enzyme releases the fluorophore; therefore, at each cycle, after irradiation of the sample, a fluorescence is emitted in a quantity proportional to the target DNA, which becomes easily quantifiable. The PCR mix is composed of: template DNA, pair of primers, dNTPs, enzyme polymerase and water up to a final volume of 20 µl. Total RNA from N2A LRP8-ddk-myc cells was isolated using TRIzol reagent (Invitrogen, USA) and then used as a template for reverse transcription with High-Capacity cDNA Reverse Transcription Kit (Applied Biosystems, USA). RT-PCR was performed using ABI PRISM 7900HT platform (Applied Biosystems, USA).

In this thesis the RT-PCR was carried out using the cDNA of BACE1: primers (forward primer 5'-GTCACTGTGCGTGCCAACA-3', reverse primer 5'-GGCCTGGCAATCTCAGCAT-3') and probe (FAM-VIC-TGCTGCCATCACTG-MGB) were appropriately designed and produced (Metabion, Germany). The normalization was done using the housekeeping genes coding for GAPDH and Actin: genes, accession numbers and probes localization are given in **Table 2**.

The samples were run in triplicate in each experimental set under standard amplification conditions up to 45 amplification cycles (Intrieri et al., 2010). Data collection was set at the annealing/extension step (60°C) [66]. Primary analysis was done within the SDS 2.3 data

collection software. Secondary analysis was done within the Relative Quantification Manager 1.2 (Applied Biosystems, USA). Relative quantization was obtained using the ΔΔCt method. (Livak and Schmittgen, 2001). The graphic was created using GraphPad Prism (v.8; GraphPad Software, USA).

Table 2 - TaqMan gene expression assays

Gene Name	Assay ID	Accession number	Exon-exon boundary	Amplicon length (bp)
GADPH	Mm99999915_g1	NM_001289726.1	4	80
Actin	Mm02619580_g1	AK075973.1	3	143

Statistical analysis

Data are reported as the mean value ± standard error of the mean (SEM) and statistical significance was examined using the Student's t-test or the One-way ANOVA test followed by Dunnett's post hoc test according to the number of the groups analyzed, respectively two or more than two. In both tests, a p value less than or equal to 0.05 (*=p<0.05; **=p<0.01; ***=p<0.001; ****=p<0.0001) was considered statistically significant (C.I. 95%). All the analyses were performed using GraphPad Prism (v.8; GraphPad Software, USA).

RESULTS

Ex vivo analysis in human brain of LRP8 processing: increase of LRP8 signal in the nucleus of neurons of AD patients.

We have previously analyzed by IHC slices of human brain from normal, non demented subjects and from AD patients, showing a clear neuronal and dendritic localization of LRP8 (detected with our home-made antibody GS1 that recognizes a specific epitope in C-terminus of LRP8: DEDELHIGRTAQIG) in both cases. However intensity and localization analyzed using confocal images showed a straight difference between controls and AD subjects: while in controls (**Fig. 5A**) the staining with the antibody GS1 showed a strong neuronal somatic and dendritic signal, besides a diffuse scattered signal in the parenchyma (likely synaptic and dendritic), on the contrary, in AD samples (**Fig. 5B**) , we observed a reduced neuronal and parenchymal signal as well as the presence of a nuclear staining mainly observable in NFTs-bearing neurons. Nuclear signal is particularly evident in cortical sections from familial AD (**Fig. 5C**), in which the severity of the disease is significant and where GS1 staining, a part the nuclear component, is significantly reduced also into the somato-dendritic compartments. Previous experiments made in our lab by SDS-PAGE and Western Blot (WB) experiments on human frozen cortical sections, revealed that in AD patients (in this case Familial subjects carrying PS1 mtations) upon immunoprecipitation of LRP8 (**Fig. 6**) there is significant increase of the C-terminal fragments corresponding to the intracellular domains (therefore named LICDs), in comparison to controls. These fragments were detected using the same specific polyclonal antibody (GS1) used previously in IHC.

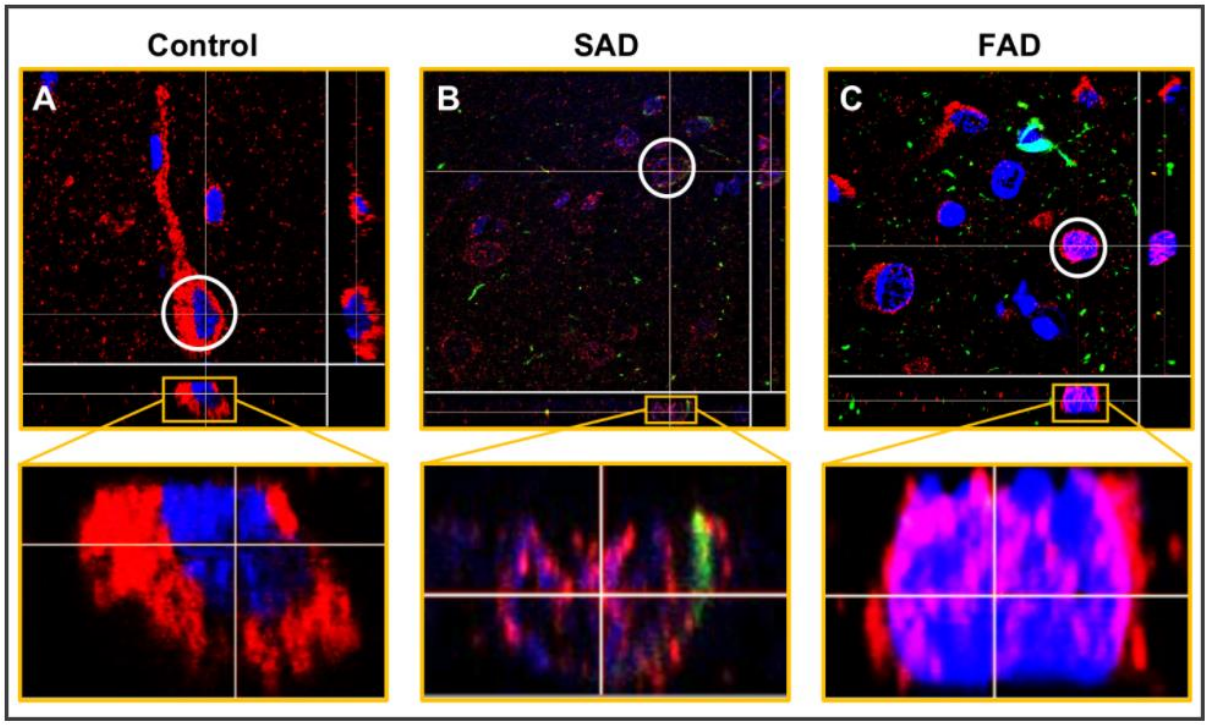

Fig. 5 - Neuronal localization of LRP8 (red) in cerebral cortex of control (A), SAD (B) and FAD (C) patients. The LRP8 staining (detected with GS1 antibody) is localized in the soma and in the processes of control neurons, whereas the LRP8 localization is more diffused in SAD and FAD brain. The magnification shows that in control neurons there is no signal of LRP8 in the nucleus; conversely, in SAD, and more severily in FAD, the nuclear localization is patent. In green tau NFTs (detected by AT100 antibody) and in blue cell nuclei stained by DAPI.

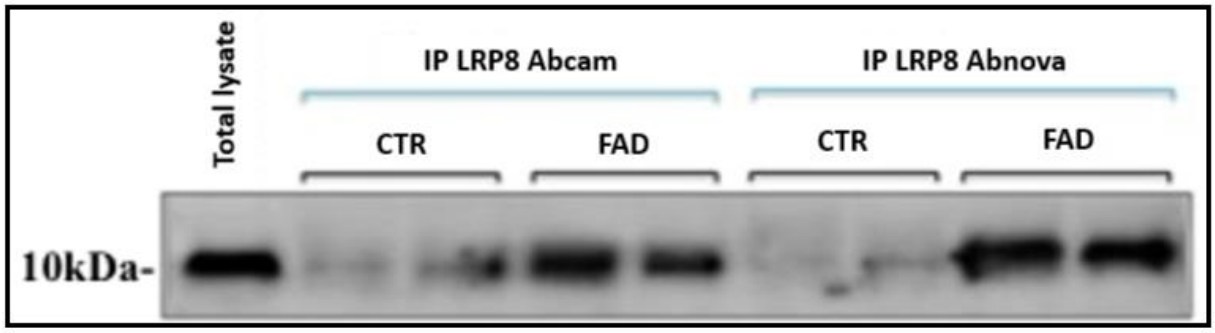

Fig. 6 - C-terminal fragments of LRP8 (LICDs). C-terminal fragments of LRP8 are detected by SDS-PAGE and Western blotting using the antibody GS1 upon immunoprecipitation by the above indicated antibodies for LRP8. In FAD (familial subjects with a PS1 mutation) there is a significant presence of LICDs, which are much less abundant in controls (CTR).

These data suggest that a different fragmentation and processing might occur in AD subjects, possibly affecting the signalling activity of LRP8.

Altogether this information prompted us to investigate the nuclear signalling of LRP8 previously reported in the literature, although in few reports.

In vitro **investigation: DAPT increases LICDs at nuclear level (SDS-PAGE and WB).**

We thus settled an *in vitro* model, using Neuro 2A (N2A) cells stably transfected with human LRP8 bearing a C-terminal ddk-myc tag (LRP8-ddk-myc), to investigate processing and localization of LRP8.

It is known from the literature that DAPT, an inhibitor of the γ-secretase complex, blocks the processing of APP's C-terminal fragments (C99/89/83), and therefore the formation of Aβ peptides. We used DAPT in the same conditions to ascertain the effect of a complete block of γ-secretase, mimicking thus a sort of "loss of function", for LRP8. We also fractionated cells using a specific "Qproteome Cell Compartment Kit" (Qiagen, Germany) to analyze also the nuclear fraction, in order to verify a possible localization of LICDs at this level.

N2A LRP8-ddk-myc cells were then treated with DAPT 10 μM O/N and total lysates, cytosolic and nuclear fractions were analyzed by Tris-Tricine SDS-PAGE followed by Western blotting (as described in Materials and Methods). LRP8 bands were identified by GS1 antibody, using as housekeeping reference the proteins β-tubulin, Histone H3 and the Lamin B1 (the last two used as nuclear markers). Densitometric analysis by informatics tools (NineAlliance, Uvitec) was performed to the quantification of each band.

The effect of γ-secretase inhibition by DAPT (positive control) was assessed by using an antibody anti C-terminus of APP (Zymed): in DAPT-treated cells we observed an increment of APP fragments migrating at 12 kDa (C99 fragment), which represent the main substrate of γ-secretase in these cells after β-secretase cleavage. As expected, the accumulation of C99 is a marker of γ-secretase inhibition (**Fig. 7, Panel A**).

DAPT treatment on N2A LRP8-ddk-myc cells showed an increase of LICDs, detected with GS1 antibody in cells' lysate, cytosol, and in nuclear extracts in comparison to the vehicle-treated cells (DMSO), while the LRP8 full length (~100 kDa) is maintained more or less at the same levels, demonstrating the DAPT influence on LRP8 fragments substrates of γ-secretase but not to the LRP8 full-length (**Fig. 7, Panel B**).

Densitometric analysis by informatics tools (NineAlliance, Uvitec) of LICDs bands, normalized for Histone H3 as housekeeping reference protein showed that the increase of the nuclear LICDs caused by DAPT is statistically significant ($p<0,05$): the average value for non-treated cells is 0,60(±0,11), whereas in N2A cells treated with DAPT is 1,01(±0,24) (**Fig. 8**).

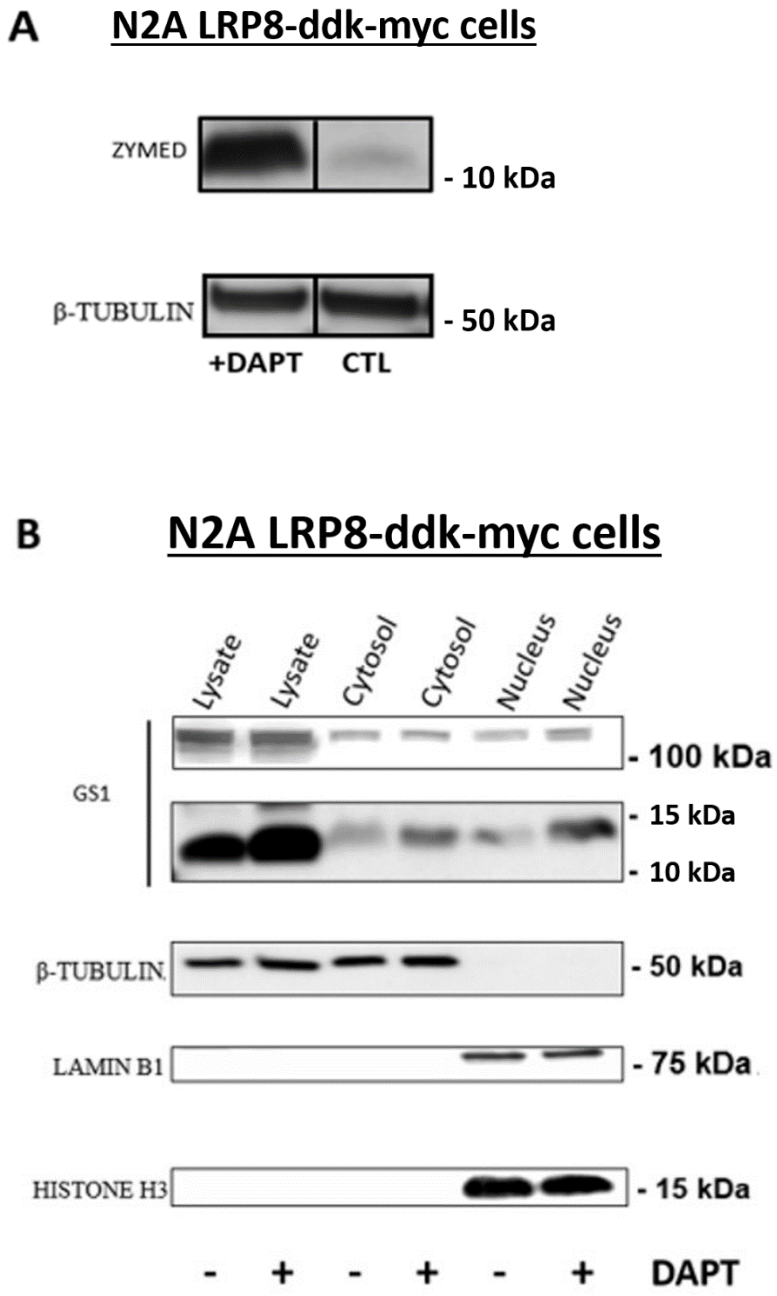

Fig. 7 - WB from N2A cells, stably expressing LRP8-ddk-myc, treated with DAPT.

Panel A: upper WB is probed with an anti C-terminus of APP (Zymed), for APP and its C-terminal fragments (C99) identification: the accumulation of C99 (at ~12kDa) in N2A LRP8-ddk-myc cells treated DAPT (10 µM, 16 hrs) highlights the occurred inhibition of γ-secretase. Lower WB is probed with β-tubulin, as housekeeping reference protein.

Panel B: Lysate, cytosol and nucleus of N2A LRP8-ddk-myc cells, previously treated with DAPT (10 µM, 16h): the blot probed with GS1 antibody shows the increase of LICDs (at ~ 10kDa) into the nucleus (and lysate and cytosol as well) in DAPT-treated cells. Interestingly, the levels of LRP8 full length (~ 100 kDa) are the same in DAPT-treated and control cells, underlining that DAPT exerts its effect on LRP8 processing and likely not on LRP8 formation. The absence of β-tubulin signal in the nuclei and the absence of the signal of Lamin B1 and Histone H3 in Lysates (and cytosol) prove that the nuclear extraction process with "Qproteome Cell Compartment Kit" was successfully achieved.

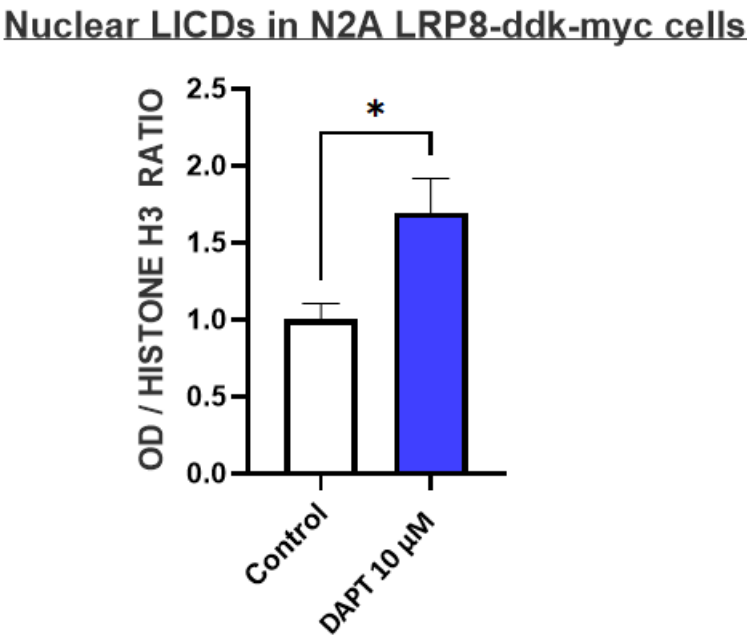

Fig. 8 - Densitometric analysis of nuclear LICDs levels in N2A LRP8-ddk-myc cells treated with DAPT 10µM. Densitometric analysis reveals a significant increase (with Student's t-test analysis) of LICDs signal in the nucleus of DAPT-treated compared to Control cells.

In vitro investigation: DAPT increases LICDs at nuclear level (Immunocytochemistry and Confocal analysis).

In order to investigate the presence of nuclear LICDs, in parallel to SDS-PAGE and WB analysis, we performed Immunocytochemistry (ICC) experiments on N2A LRP8-ddk-myc cells treated with DAPT (as described in Materials and Methods section).

N2A LRP8-ddk-myc cells show a very intense staining on cell surface structures and in cell arborization, which is significantly enhanced in comparison to parental control cells (not shown). It is also observable a nuclear localization of GS1 staining, which is higher in N2A cells treated with DAPT in comparison to vehicle-treated cells (**Fig. 9**).

It seems therefore that the complete inhibition of γ-secretase induces an increment of nuclear LRP8 signal, as also shown by SDS-PAGE and WB where we detected an increase of LICDs at nuclear level upon DAPT treatment.

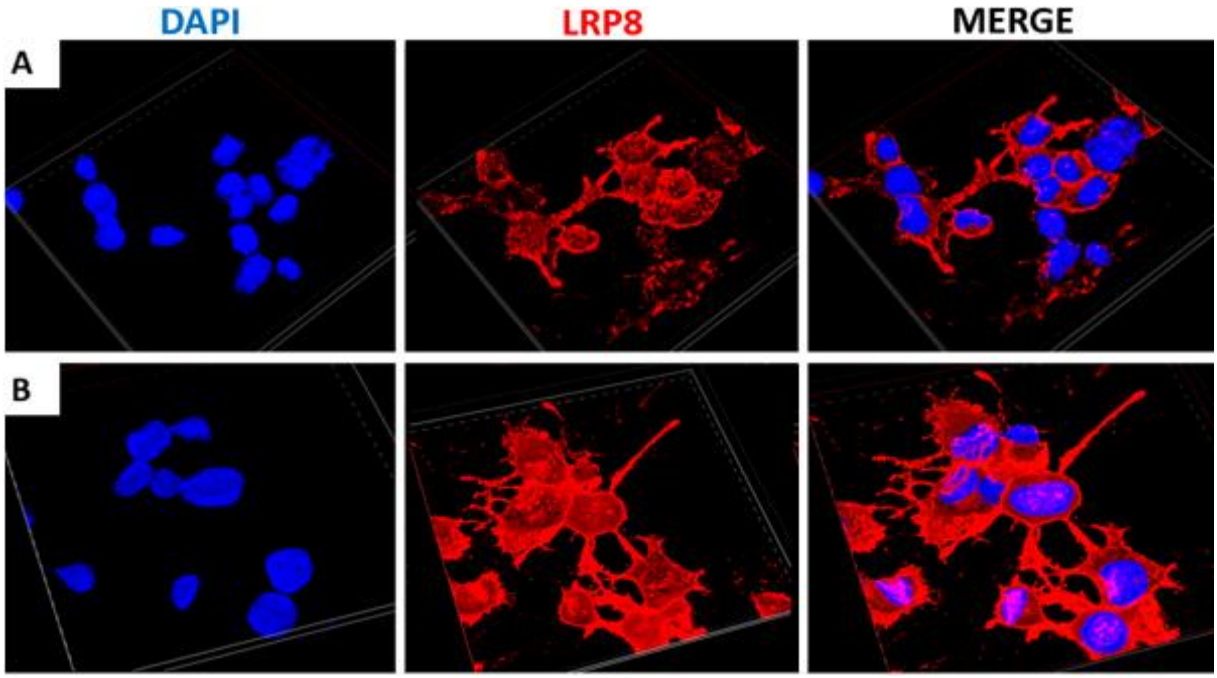

Fig. 9 - Immunocytochemistry analysis of LRP8 (red) and DAPI (blue, for nuclear staining) on N2A LRP8-ddk-myc cells treated with DAPT. The DAPT-treated cells (**Panel B**) display an increment of nuclear LRP8 staining (detected with GS1 antibody) compared to control cells (**Panel A**).

Reduction of C-terminal fragments of LRP8 intracellular domains (LICDs) in N2A cells by Actinonin and by anti-LRP8 antibody (Ab).

Our previous studies in brains from AD patients showed that there is an increase of mRNA and protein levels of different proteases with a putative role in AD [67]. Among them, Meprin β is a candidate to generate N-terminally truncated of Aβ (in particular Aβ2-40) peptides [23]. In this case we decided to use Actinonin, which is a potent and reversible inhibitor of MMP-1, MMP-3, MMP-8, MMP-9, and Meprins with Ki values of 300 nM, 1,700 nM, 190 nM, 330 nM, and 20 nM, respectively, to test whether this small molecule could interfere with LRP8 processing and LICDs generation [68].

To this end, we treated N2A stably transfected with LRP8 ddk-myc with increasing concentrations (50, 100, 200 μM) of the drug for a 16h (as described in Materials and Methods). The putative inhibitory activity of Actinonin was verified upon SDS-PAGE and WB experiments, by using the GS1 polyclonal antibody for the detection of LICDs and β-tubulin as housekeeping reference protein.

WB experiments show that the higher is the concentration of Actinonin used the greater is the LICDs reduction (**Fig. 10**). The densitometric analysis reveals a statistically significant reduction (with a $p<0,0001$ calculated with Anova test) of the LICDs, proportional to the concentration of Actinon used (**Fig. 11**).

These results highlighted that the inhibitory activity of Actinon on MMPs or on Meprin β induces a reduction of LICDs, suggesting an involvement of these proteases on the LRP8 cleavage.

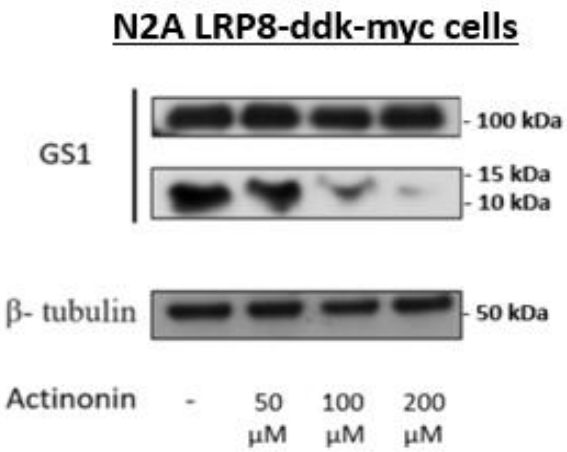

Fig. 10 - WB of N2A LRP8-ddk-myc cells lysate treated with increasing concentrations of Actinonin. WB, probed with GS1 antibody for the detection of LRP8, shows that the higher is the Actinonin concentration, the greater is the LICDs reduction (at ~ 10 kDa), with a maximum of inhibitory efficacy with Actinonin 200 µM; note that no differences in LRP8 full-length (~ 100 kDa) between treated and control cells are observed. Lower WB is probed with the housekeeping reference protein β-tubulin.

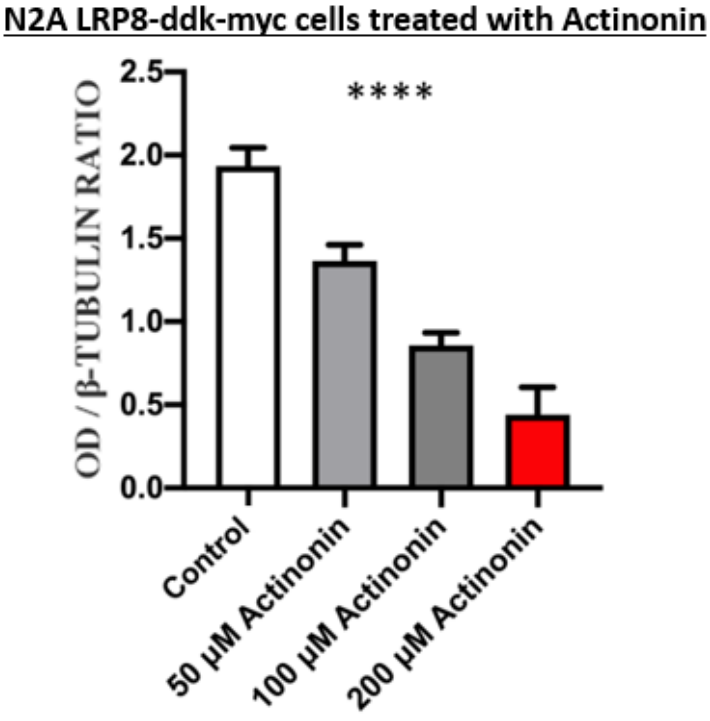

Fig. 11 - Densitometric analysis of lysate of N2A LRP8-ddk-myc cells treated with Actinonin 50, 100 and 200 µM. The densitometric analysis shows that the Actinonin causes a reduction of LICDs corresponding to the concentration of the drug used. The average values (normalized for the β-tubulin protein) are 1,935(±0,2186) for Control cells, 1,365(±0,1914) for cells treated with Actinonin 50 µM, 0,8575(±0,15119) with Actinonin 100 µM and 0,4400(±0,3318) with Actinonin 200 µM.

To verify if the decrease of LICDs induced by Actinonin would affect also the nuclear pool of LICDs, we extracted and solubilized nuclear proteins from N2A LRP8-ddk-myc cells, using the "Qproteome Cell Compartment Kit" (Qiagen), according to the procedure described in *Materials and Methods.*

We decided to use Actinonin 200 µM, since it was the more effective concentration in LICDs reduction (as described in the previous section): cells were cultured in t75 Flask until to ~70% of confluence and treated with Actinonin 200 µM for 16 h. Subsequently lysate and cytosolic and nuclear fractions were analyzed by SDS-PAGE and WB analysis with the antibody GS1.

WB experiments reveal that the signal corresponding to the main LICDs fragment, detected with GS1 antibody, is significantly reduced into the nucleus, as well as in the lysate and cytosol **(Fig. 12)**

Densitometric analysis by informatics tools (NineAlliance, Uvitec) of LICDs bands, normalized for Histone H3 as housekeeping reference protein, shows that the reduction of nuclear LICDs caused by Actinonin is statistically significant ($p<0,01$): the average value for non-treated cells is 1,010(±0,07), whereas in N2A cells treated with Actinonin is 0,683(±0,08) (**Fig. 13**). Therefore, these experiments suggest a possible role for MMPs or Meprin β in LRP8 processing, rather that γ-secretase, since Actinonin does not inhibit this enzyme.

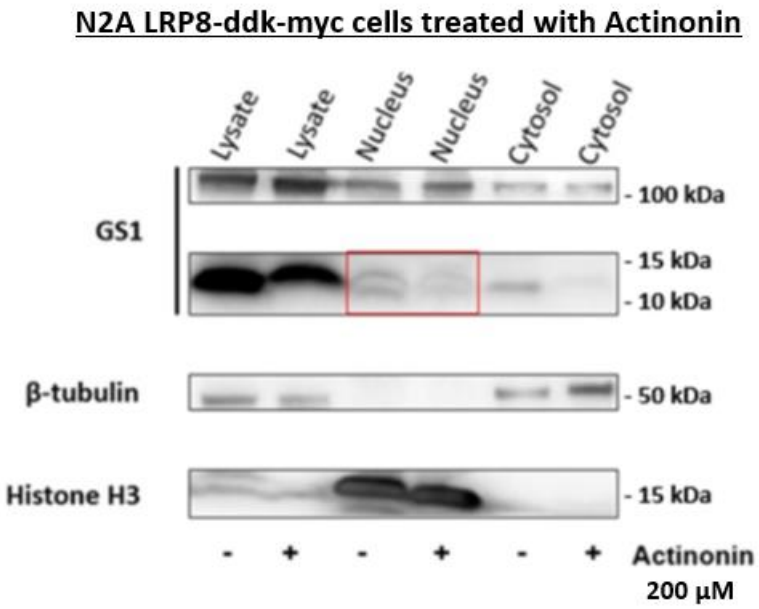

Fig. 12 - WB of lysate, nucleus and cytosol of N2A LRP8-ddk-myc cells treated with Actinonin. WB analysis displays the LICDs (at ~10 kDa) reduction in nucleus (red rectangle), detected with GS1, as well as in cytosol and lysate. The absence of β-tubulin signal and, conversely, the Histone H3 signal in nuclei, prove that the nuclear extraction was successfully achieved.

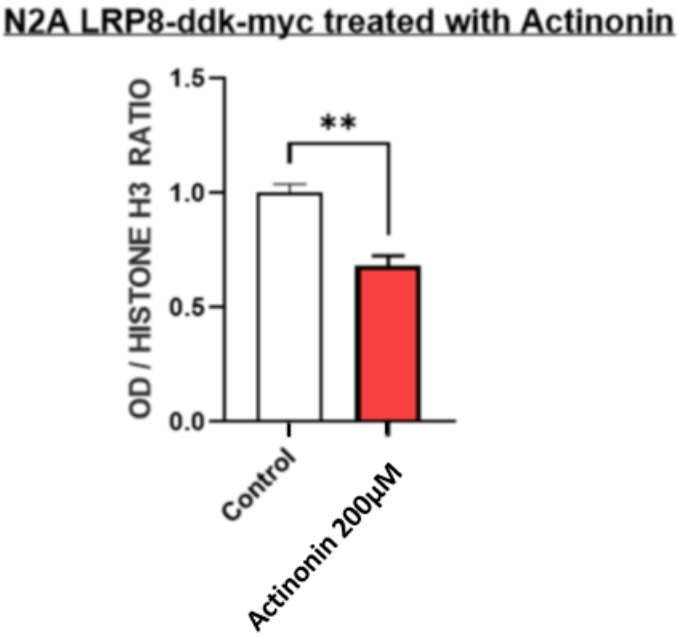

Fig. 13 - Densitometric analysis of nuclear LICDs levels in N2A LRP8-ddk-myc cells treated with Actinonin 200 µM. Densitometric analysis reveals a significant decrease (with Student's t-test analysis) of LICDs signal in the nucleus of Actinonin-treated cells compared to Control cells.

We then analyzed nuclear LICDs on N2A LRP8-ddk-myc cells upon challenge with Actinonin, in ICC experiments.

Immunocytochemistry analysis reveals that in N2A cells treated with Actinonin 200 µM the nuclear signal of LRP8, detected with GS1 antibody, is significantly reduced in respect to that detectable in vehicle-treated cells. (**Fig. 14**).

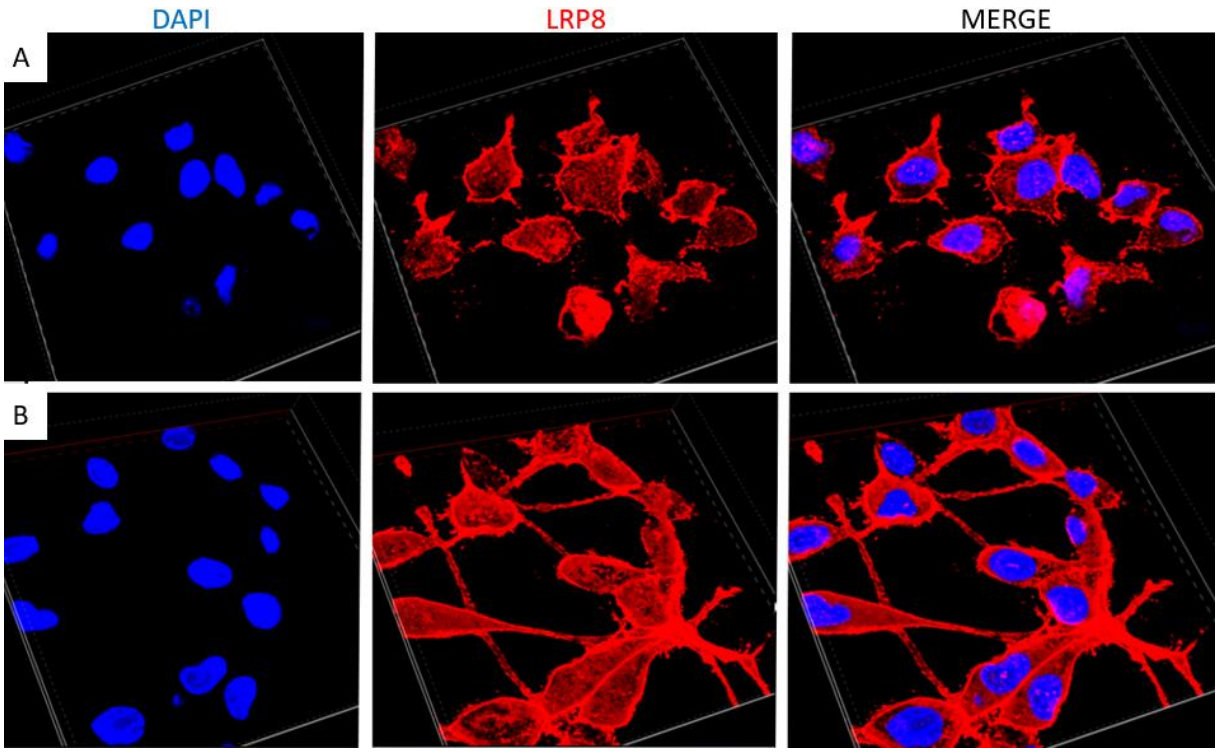

Fig. 14 - Immunocytochemistry analysis of LRP8 (red) and DAPI (blue, for nuclear staining) on N2A LRP8-ddk-myc cells treated with Actinonin 200 µM. The Actinonin-treated cells (**Panel B**) show a reduction of nuclear LRP8 (detected with GS1 antibody) staining compared to control cells (**Panel A**).

As further control, we treated N2A cells expressing LRP8-ddk-myc with an antibody specific for the N-terminus of LRP8 (Ab), aiming at reducing endocytosis and processing of the receptor. Effectively, as shown in **Fig. 15**, we observed a reduction of LICDs in Ab-treated cells, and in parallel a reduction of nuclear signal detected by ICC using GS1 antibody and confocal imaging (**Fig. 16**). Focusing at nuclear plane, we can observe a significant inhibition of nuclear presence of red-signal on Ab-treated cells (B), in comparison to untreated cells (A).

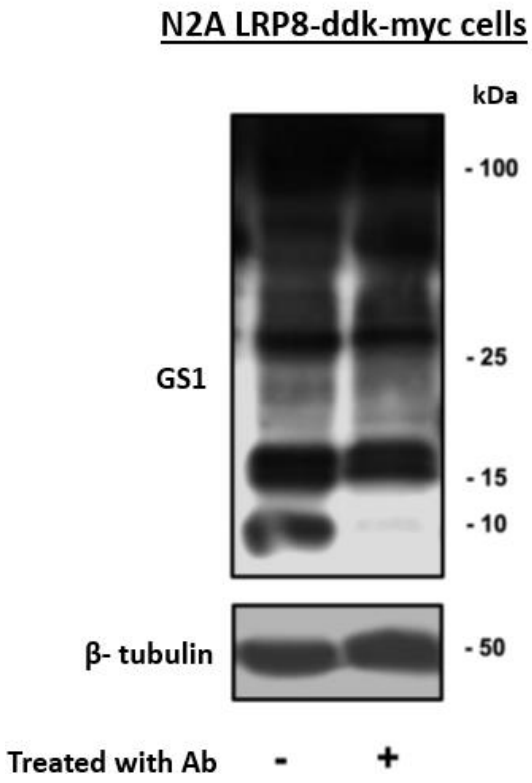

Fig. 15 - WB of cell lysate from N2A LRP8-ddk-myc cells. Cell were challenged with the antibody Ab specific for the N-terminal portion of LRP8 (3hr, 1µg/ml) and then, upon cell lysis, proteins were analyzed by Tris-tricine SDS-PAGE and WB using GS1 antibody. β-tubulin is shown as loading control.

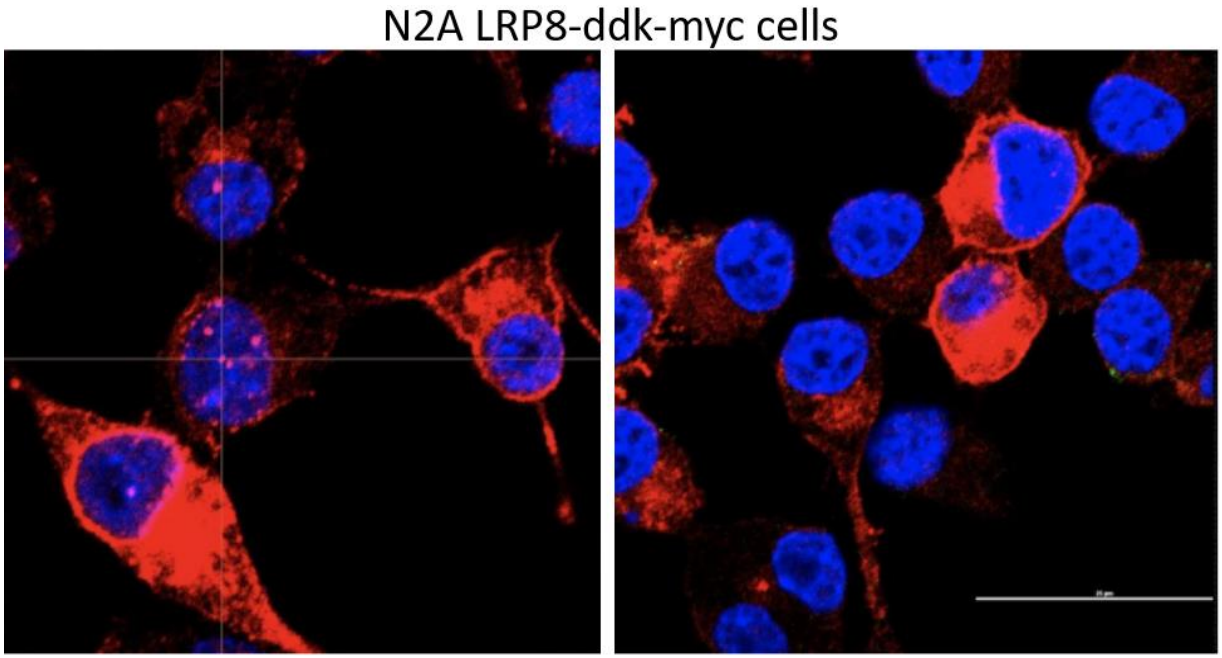

Fig. 16 - Immunocytochemistry analysis of LRP8 (red) and DAPI (blue, for nuclear staining) on N2A LRP8-ddk-myc cells treated with the antibody Ab for the N-terminus of LRP8, using the same conditions as for WB (1µg/ml, 3 Hrs). Ab-treated cells (**right panel**) show a reduction of nuclear LRP8 staining compared to control cells (**left panel**). (Scale bar: 35 µm).

Altogether these data show that the formation of LICDs can be modulated either using small drugs (DAPT, Actinonin) or even antibodies for LRP8. The processing of LRP8, which is apparently upregulated in AD conditions, and the nuclear content of its LICDs could be therefore reduced in certain conditions.

Significance of LICDs and possible role in AD development.

The presence of LICDs at nuclear level may have a significance in AD if is linked to translational effects over the genes involved in AD such as APP and BACE1. We therefore decided to look at mRNA levels of these genes in cells expressing LRP8 or its C-terminal fragments encoded by a cDNA trancribing the following sequence:

CMSGYLIWRNWKRKNTKSMNFDNPVYRKTTEEEDEDELHIGRTAQIGHVYPAAISSFDRPLWAEPCLGE TREPEDPAPALKELFVLPGEP RSQLHQLPKNPLSELPVVKSKRVALSLEDDGLP, therefore maintaining the entire C-terminal portion of the receptor. This construct (named C12) has a processing similar to that of LRP8 as shown in **Fig. 17.**

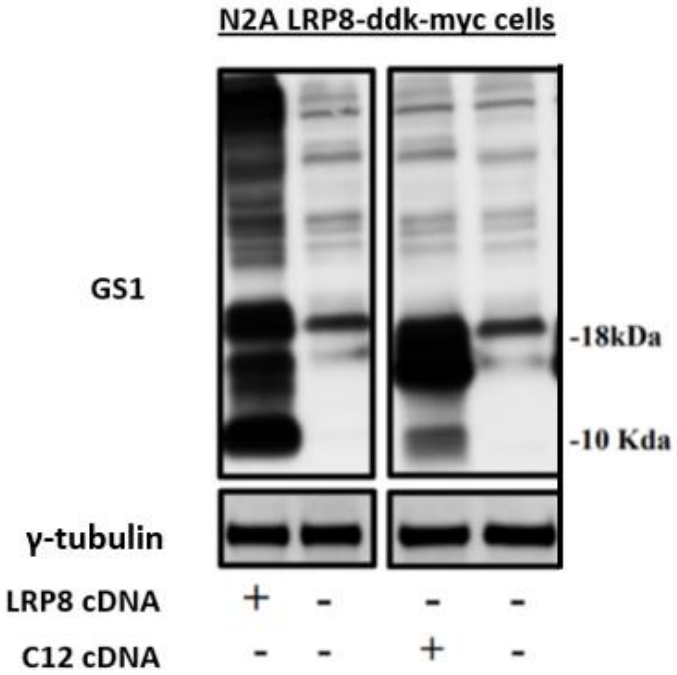

Fig. 17 - WB of cell lysate from N2A LRP8-ddk-myc cells *(Adapted from a Doctoral thesis of our lab)*. Cell were tranfected either to express LRP8 or its C-terminal fragment C12 and then, upon cell lysis, proteins were analyzed by Tris-tricine SDS-PAGE and WB using GS1 antibody. γ-tubulin is shown as loading control.

We therefore measured by RT-PCR the relative content of mRNA of BACE1 and APP in cells expressing LRP8 or C12, hypothesizing a transcriptional role of this protein directly over those genes which have likely a pivotal role in AD development. In these experiments, we did not observe significant variations on APP's levels mRNA, while we observed a significant increment of BACE1's mRNA in both cells expressing LRP8 or C12. The effect of C12 on BACE1 was very relevant, since reached almost 3,5-fold increment over wild type cells as shown in **Fig. 18.**

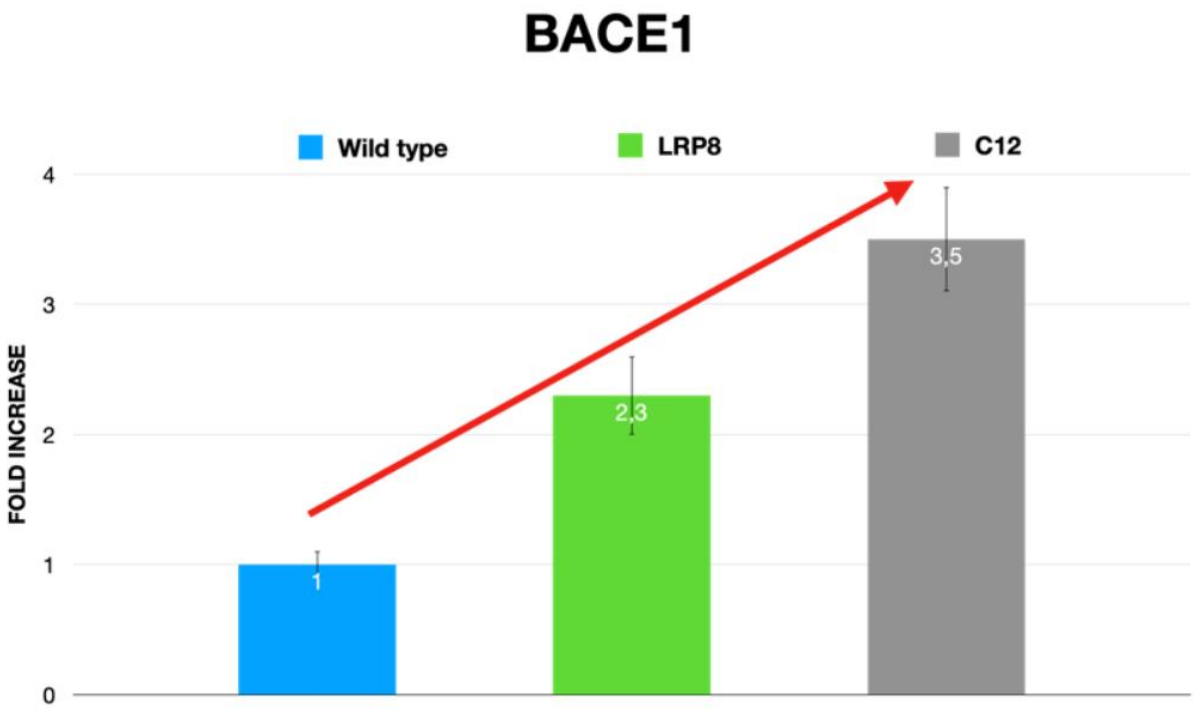

Fig. 18. RT-PCR of N2A WT cells (pale blue), expressing LRP8 (green) and expressing C12 (grey). The mRNA levels of BACE1 are increased 2,3-fold in N2A cells expressing LRP8 and 3,5-fold in N2A cells expressing the C12 construct , in comparison to N2A WT cells.

DISCUSSION

The amyloid cascade hypothesis was for more than 25 years the main model to explain the pathogenesis of Alzheimer's disease (AD), also addressing the pharmaceutical treatments for AD [27][28]. However, problems have been raised about the "amyloid only hypothesis" (see Introduction) and the clinical failure of trials based on amyloid cascade hypothesis have cast considerable doubt on its reliability.

We focused our attention on LRP8 receptor since we think that it can have a contribution in AD onset, in that it shows several connections with AD: it is expressed in brain, in particular at neuronal level [45]; it is involved in learning and memory processes, by mediating the Reelin pathway and modulating NMDA receptors function [58][59]; LRP8 interacts with APP and they mutually affect their processing; LRP8 shares with APP extracellular proteins (such as F-Spondin) and intracellular adaptors (such as FE65 and Dab1) modulating the processing and the pathway of both receptors [62][63][51][58][52]; moreover, LRP8 is the main neuronal receptor for ApoE, the most important risk factor to develop AD.

Our studies, conducted on brain from control non-demented subjects and from AD patients, allowed to verify the expression pattern and processing of LRP8: by Immunohistochemistry (IHC) experiments we identified a specific reduction of axonal and dendritic localization, with a parallel increment of a nuclear localization of LRP8 in AD patients; by SDS-PAGE and Western Blot (WB) experiments we evidenced a reduction of full length receptor and a parallel increment of C-terminal fragments in AD and FAD patients, in comparison to controls. Altogether, these data suggest that in course of AD may occur an increment of processing along with a re-localization of C-terminal fragments. From the literature is known that LRP8 is cleaved by the same proteases that cut APP: of particular importance is the γ-secretase cleavage, because it releases the C-terminal fragments of APP with a likely transcriptional role, and in parallel produces Aβ peptides. It is still debated whether the hypothetical "loss-of-

function" of γ-secretase causes dementia and neurodegeneration in AD [34][35] through Aβ or through a different mechanism. If LRP8 has a role in AD it could be related either to its interaction with APP, or through ApoE, or because interferes with γ-secretase cleavage. Apparently, in AD and FAD patients there is a clear scenario in which LRP8 has a different processing and localization in respect to non-AD subjects. These situations prompted us to investigate its processing and localization *in vitro*, to better understand the biochemical mechanisms in which it can be involved.

From the point of view of LRP8 however the question is peculiar because it has direct and indirect linkage with all the genes pivotal in the genesis of AD. In fact, considering the known genetic causes of FAD, which could be the role of LRP8? If we consider that APP overexpression causes AD (this is verified in Down Syndrome cases as well as in familial patients with mutations in the promoter region of APP which enhance APP's transcription), what could be the consequences of higher APP (C99/83) levels on LRP8? Considering Presenilin's mutations (the γ-secretase's catalytic protein), which could be the consequences on LRP8 (which is a substrate of the enzyme)? And finally, ApoE e4, how could it modulate or get an influence over LRP8?

In our lab, in these years we investigated these questions and we obtained some answers:

1- we have data showing that APP and its CTFs (C99/C83 mainly) when overexpressed induce a significant increment on LICDs, the same phenotype observed in AD brains;
2- when γ-secretase is blocked with inhibitors such as DAPT, or even absent, such as in KO cells, the level of LICDs is enhanced;
3- ApoE e4 changes the sorting of LICDs and CTFs, enhancing their localization in exosomes.

In this study we investigated the nuclear presence of LRP8 C-terminal fragments, in particular of LICDs (detected at around 8-12kDa). A nuclear component of LRP8 is present in AD and FAD patients (as shown in **Fig. 5**), however we do not have yet the evidence that this nuclear pool is made exclusively of LICDs (as *in vitro* studies seems to suggest) since nuclear preparations from human brains are difficult to obtain with a high degree of purity. Our *in vitro* analysis shows that a pool of LICDs can be isolated also in nuclear fractions and that this pool is even enhanced upon inhibition of γ-secretase (DATP treatments, see **Figs.7-9**). We thus hypothesize that in a scenario of γ-secretase's loss of function, LICDs levels increase as well as their re-localization on cellular compartments such as nucleus and exosomes. In fact, we have evidence (not shown in this study) that DAPT may increase also the exosomal content in C99 and LICDs. These peculiar features triggered by DAPT treatment might explain the reason why clinical trials based on γ-secretase's inhibition or modulation failed, even when effectively Aβ peptides were reduced and plaques formation hampered.

In this scenario our hypothesis is that either APP overexpression and a partial or complete "loss of function" of γ-secretase modulate the processing of LRP8 toward an increased formation of LICDs that are misplaced in cell nuclei and exosomes. In this work we also provide evidence that the C-terminal portion of LRP8, likely through its nuclear localization, may trigger a vicious loop enhancing the transcription of BACE 1, the enzyme responsible of C99/C89 formation. In this sense a higher level of C99 may further compete with LRP8 processing, leading to an accumulation of LICDs in a circular manner.

These speculations however can be definitely proven only knowing the exact sequences hidden in LICDs fragments. Our data suggest that LICDs level is increased by blocking γ-secretase, therefore implying that the sequence should contain the transmembrane region where the cleavage site is embedded. Otherwise, we should assume that when γ-secretase is

hampered, other proteases are recruited cleaving the 25kDa precursor at a different site. Moreover, the molecular weight observed (at around 10 kDa) even in C12-expressing cells (**Fig. 17**) suggests that these fragments undergo a further C-terminal processing.

If confirmed, the hypothesis of a "loss of function" of γ-secretase would have an advantage over the "alternative enzyme" hypothesis that would come into play when γ-secretase is blocked. Furthermore, it would also be easier to explain the rise of LICDs levels when APP/C99 are upregulated: simply on a competitive basis versus the enzyme.

The "alternative enzyme" hypothesis is also very interesting from a different point of view: in fact, the C-terminal portion of LICDs is undoubtably cleaved on the contrary to what happens to AICDs, generated from APP C-terminal region. In fact, a part the observation in **Fig. 17,** we have data presented in previous work, using other C-terminal antibodies, showing this peculiar feature. Therefore, while C99 generates AICDs only upon γ-secretase cleavage, the C-terminal portion of LRP8 is processed necessarily by two enzymes: γ-secretase and a second cleavage closer to the C-terminus. We do not have at present evidence of smaller fragments of LICDs detectable with C-terminal antibodies or with specific antibodies for the ddk-myc tag in our experiments (personal observation), suggesting that the very C-terminal portion is degraded after being cleaved.

In any case the need for two enzymatic cuts suggests a very complex processing conditioned by several enzymes. In fact, in this study we also provide evidence that the generation of LICDs can be modulated and even blocked either using an antibody vs the N-terminus of LRP8 (**Figs. 15 and 16**), or using a small molecule such as Actinonin (**Figs. 10-14**): a rather specific inhibitor of Metalloproteases and of Meprin, the latter being involved also into the processing of APP. The relative absence of LICDs (even the nuclear pool) using this drug suggests that other enzymes, apart from γ-secretase, come into play and, in our case, may even intervene before

the γ- cut, as also suggested by the experiments using DAPT and in which the LICDs migrate at their molecular weight defined independently of γ-secretase cleavage. Therefore, the C-terminal enzymatic cleavage may precede, or even predispose and be necessary, for the subsequent cleavage by γ-secretase. The good news is that the formation of LICDs can be hampered, and therefore, should their pathogenetic role be confirmed, a therapeutic intervention could be hypothesized, using antibodies toward the N-terminus of LRP8 or even small molecules derivable from Actinonin. Certainly, we need to deepen the studies regarding the possible role of other enzymes, identifying exactly which they are, in order to act in a more specific way to modulate the processing of LRP8.

Since in the literature mRNA expression and protein levels of selected proteases involved in APP processing and with a putative role in AD (such as Meprin β) was found increased in the brain of AD subjects [67], we cannot exclude that in pathogenetic conditions an increment of selected protease's activity (besides γ-secretase, which instead should work with less efficiency in AD) may further enhance LICDs.

In this thesis is also shown a possible pathogenic role exerted by the C-terminal portion of LRP8 if upregulated. Using the C12 construct we show that this one can be cleaved to form LICDs and that both LRP8 and C12 upregulate the mRNA level of BACE1, leaving unaltered APP's mRNA. Therefore, the transcriptional role of LRP8 might be linked to the regulation of BACE1 levels (which in some papers were found enhanced in AD patients [69] [70]) with a clear relevance for AD. In fact, BACE1 is the pivotal enzyme responsible for the generation of C99 and C89 fragments, substrates of γ-secretase, considered amyloidogenic (are the precursors of Aβ1-40/42 and Aβ11-40/42) and *per se* neurotoxic in transgenic mice [71]. Therefore, in the view of the "amyloid hypothesis," the processing of LRP8 toward an increment of the nuclear pool of LICDs might further enhance the amyloidogenic processing

of APP and contribute to amyloidosis in AD. From the point of view of LRP8, however, the effect over BACE1 and a likely increment of C99/C89 could be equally negative, as it could increase the effect of C99 on the processing of LRP8 (probably on a competitive basis), further increasing the formation of LICDs in a vicious pathogenic loop. Furthermore, considering the presence of LICDs and of C99 in the secreted exosomal compartment (when overexpressed), we could also hypothesize that these fragments may also contribute to diffuse the information to neighboring neurons, contributing to the spread of the disease in an amyloidogenic sense. In this scenario, the role of LRP8 could therefore be linked to a further increment of amyloid formation in the brain.

Finally, there is to define the role of ApoE. LRP8 is the main neuronal receptor for ApoE and in our lab we have evidence, yet unpublished, showing that ApoE e4 is able to sort LICDs to exosomes, while ApoE e2/3 are much less efficient. In our hypothesis therefore the role of ApoE e4 may be relevant only regarding the putative role in the interneuronal diffusion of the information carried by LICDs.

We are planning to verify whether ApoE could affect LICDs as far as it concerns their nuclear localization and their transcriptional activity. In this case our hypothesis could imply a role of Apo Ee4 again in an amyloidogenic sense: not so much for its ability to bind Aβ, but rather modulating the transcriptional activity of LRP8, through its LICDs, raising the levels of BACE1, and consequently of C99, and thus increasing the amyloidosis through a different, parallel mechanism. In any case, these pathways could be blocked by using antibodies to LRP8 or molecules such as Actinonin, as here shown.

Altogether our study suggests that the receptor LRP8, being at the intersection between the different genetic components of the disease, could contribute in a pathogenetic sense to the spread of the disease and, indirectly, to amyloidosis through different pathways. In this work

we have examined only the possible nuclear contribution of LRP8's fragments to the disease and how their production could be negatively regulated in a therapeutic sense.

BIBLIOGRAPHY

[1] https://www.who.int/news-room/fact-sheets/detail/dementia n.d.

[2] Dening T, Sandilyan MB. Dementia: definitions and types. Nurs Stand 2015;29:37–42. https://doi.org/10.7748/ns.29.37.37.e9405.

[3] Weller J, Budson A. Current understanding of Alzheimer's disease diagnosis and treatment. F1000Research 2018;7. https://doi.org/10.12688/f1000research.14506.1.

[4] Hippius H, Neundörfer G. The discovery of Alzheimer's disease. Dialogues Clin Neurosci 2003;5:101–8. https://doi.org/10.31887/dcns.2003.5.1/hhippius.

[5] Dumery L, Bourdel F, Soussan Y, Fialkowsky A, Viale S, Nicolas P, et al. β-Amyloid protein aggregation: Its implication in the physiopathology of Alzheimer's disease. Pathol Biol 2001;49. https://doi.org/10.1016/S0369-8114(00)00009-2.

[6] Verri M, Pastoris O, Dossena M, Aquilani R, Guerriero F, Cuzzoni G, et al. Mitochondrial alterations, oxidative stress and neuroinflammation in Alzheimer's disease. Int J Immunopathol Pharmacol 2012;25. https://doi.org/10.1177/039463201202500204.

[7] 2020 Alzheimer's disease facts and figures. Alzheimer's Dement 2020;16. https://doi.org/10.1002/alz.12068.

[8] Goedert M. Alzheimer's and Parkinson's diseases: The prion concept in relation to assembled Aβ, tau, and α-synuclein. Science (80-) 2015;349. https://doi.org/10.1126/science.1255555.

[9] Tsolaki M, Kokarida K, Iakovidou V, Stilopoulos E, Meimaris J, Kazis A. Extrapyramidal symptoms and signs in Alzheimer's disease: Prevalence and correlation with the first symptom. Am J Alzheimers Dis Other Demen 2001;16. https://doi.org/10.1177/153331750101600512.

[10] Boccardi V, Ruggiero C, Patriti A, Marano L. Diagnostic Assessment and Management

of Dysphagia in Patients with Alzheimer's Disease. J Alzheimer's Dis 2016;50. https://doi.org/10.3233/JAD-150931.

[11] Brookmeyer R, Corrada MM, Curriero FC, Kawas C. Survival following a diagnosis of Alzheimer disease. Arch Neurol 2002;59. https://doi.org/10.1001/archneur.59.11.1764.

[12] Sengoku R. Aging and Alzheimer's disease pathology. Neuropathology 2020;40. https://doi.org/10.1111/neup.12626.

[13] De Leon MJ, George AE, Stylopoulos LA, Smith G, Miller DC. EARLY MARKER FOR ALZHEIMER'S DISEASE: THE ATROPHIC HIPPOCAMPUS. Lancet 1989;334. https://doi.org/10.1016/S0140-6736(89)90911-2.

[14] Juottonen K, Laakso MP, Insausti R, Lehtovirta M, Pitkänen A, Partanen K, et al. Volumes of the entorhinal and perirhinal cortices in Alzheimer's disease. Neurobiol Aging 1998;19. https://doi.org/10.1016/S0197-4580(98)00007-4.

[15] Poulin SP, Dautoff R, Morris JC, Barrett LF, Dickerson BC. Amygdala atrophy is prominent in early Alzheimer's disease and relates to symptom severity. Psychiatry Res - Neuroimaging 2011;194. https://doi.org/10.1016/j.pscychresns.2011.06.014.

[16] Sorbi S, Forleo P, Tedde A, Cellini E, Ciantelli M, Bagnoli S, et al. Genetic risk factors in familial Alzheimer's disease. Mech. Ageing Dev., vol. 122, 2001. https://doi.org/10.1016/S0047-6374(01)00308-6.

[17] Kennedy AM, Brown J, Rossor M. The genetics of Alzheimer's disease. Baillieres Clin Neurol 1994;3. https://doi.org/10.6064/2012/246210.

[18] Zheng H, Koo EH. Biology and pathophysiology of the amyloid precursor protein. Mol Neurodegener 2011;6. https://doi.org/10.1186/1750-1326-6-27.

[19] O'Brien RJ, Wong PC. Amyloid precursor protein processing and alzheimer's disease.

Annu Rev Neurosci 2011;34. https://doi.org/10.1146/annurev-neuro-061010-113613.

[20] Jiang H, Jayadev S, Lardelli M, Newman M. A Review of the Familial Alzheimer's Disease Locus PRESENILIN 2 and Its Relationship to PRESENILIN 1. J Alzheimer's Dis 2018;66. https://doi.org/10.3233/JAD-180656.

[21] Chow VW, Mattson MP, Wong PC, Gleichmann M. An overview of APP processing enzymes and products. Neuromolecular Med 2010;12. https://doi.org/10.1007/s12017-009-8104-z.

[22] Kojro E, Fahrenholz F. The non-amyloidogenic pathway: structure and function of alpha-secretases. Subcell Biochem 2005;38. https://doi.org/10.1007/0-387-23226-5_5.

[23] Bien J, Jefferson T, Čaušević M, Jumpertz T, Munter L, Multhaup G, et al. The metalloprotease meprin β generates amino terminal-truncated amyloid β peptide species. J Biol Chem 2012;287. https://doi.org/10.1074/jbc.M112.395608.

[24] Becker-Pauly C, Pietrzik CU. The metalloprotease meprin β is an alternative β-secretase of APP. Front Mol Neurosci 2017;9. https://doi.org/10.3389/fnmol.2016.00159.

[25] Hardy JA, Higgins GA. Alzheimer's disease: The amyloid cascade hypothesis. Science (80-) 1992;256. https://doi.org/10.1126/science.1566067.

[26] Morris GP, Clark IA, Vissel B. Inconsistencies and Controversies Surrounding the Amyloid Hypothesis of Alzheimer's Disease. Acta Neuropathol Commun 2014;2. https://doi.org/10.1186/s40478-014-0135-5.

[27] Karran E, De Strooper B. The amyloid cascade hypothesis: are we poised for success or failure? J Neurochem 2016;139. https://doi.org/10.1111/jnc.13632.

[28] Ricciarelli R, Fedele E. The Amyloid Cascade Hypothesis in Alzheimer's Disease: It's

Time to Change Our Mind. Curr Neuropharmacol 2017;15. https://doi.org/10.2174/1570159x15666170116143743.

[29] Lee SF, Shah S, Li H, Yu C, Han W, Yu G. Mammalian APH-1 interacts with presenilin and nicastrin and is required for intramembrane proteolysis of amyloid-β precursor protein and Notch. J Biol Chem 2002;277. https://doi.org/10.1074/jbc.M208164200.

[30] Prokop S, Shirotani K, Edbauer D, Haass C, Steiner H. Requirement of PEN-2 for stabilization of the presenilin N-/C-terminal fragment heterodimer within the γ-secretase complex. J Biol Chem 2004;279. https://doi.org/10.1074/jbc.M401789200.

[31] Wolfe MS. Dysfunctional γ-Secretase in Familial Alzheimer's Disease. Neurochem Res 2019;44. https://doi.org/10.1007/s11064-018-2511-1.

[32] Wolfe MS. Structure and Function of the γ-Secretase Complex. Biochemistry 2019;58. https://doi.org/10.1021/acs.biochem.9b00401.

[33] Russo C, Violani E, Salis S, Venezia V, Dolcini V, Damonte G, et al. Pyroglutamate-modified amyloid β-peptides - AβN3(pE) - strongly affect cultured neuron and astrocyte survival. J Neurochem 2002;82. https://doi.org/10.1046/j.1471-4159.2002.01107.x.

[34] Russo C, Schettini G, Saido TC, Hulette C, Lippa C, Lannfelt L, et al. Presenilin-1 mutations in Alzheimer's disease. Nature 2000;405. https://doi.org/10.1038/35014735.

[35] Shen J, Kelleher RJ. The presenilin hypothesis of Alzheimer's disease: Evidence for a loss-of-function pathogenic mechanism. Proc Natl Acad Sci U S A 2007;104. https://doi.org/10.1073/pnas.0608332104.

[36] Du X, Wang X, Geng M. Alzheimer's disease hypothesis and related therapies. Transl Neurodegener 2018;7. https://doi.org/10.1186/s40035-018-0107-y.

[37] Mohandas E, Rajmohan V, Raghunath B. Neurobiology of Alzheimer's disease. Indian J Psychiatry 2009;51. https://doi.org/10.4103/0019-5545.44908.

[38] Medina M, Garrido JJ, Wandosell FG. Modulation of GSK-3 as a therapeutic strategy on tau pathologies. Front Mol Neurosci 2011;4. https://doi.org/10.3389/fnmol.2011.00024.

[39] Naseri NN, Wang H, Guo J, Sharma M, Luo W. The complexity of tau in Alzheimer's disease. Neurosci Lett 2019;705. https://doi.org/10.1016/j.neulet.2019.04.022.

[40] Mandrekar-Colucci S, Landreth GE. Microglia and Inflammation in Alzheimers Disease. CNS Neurol Disord - Drug Targets 2012;9. https://doi.org/10.2174/187152710791012071.

[41] Frost GR, Li YM. The role of astrocytes in amyloid production and Alzheimer's disease. Open Biol 2017;7. https://doi.org/10.1098/rsob.170228.

[42] Bolós M, Perea JR, Avila J. Alzheimer's disease as an inflammatory disease. Biomol Concepts 2017;8. https://doi.org/10.1515/bmc-2016-0029.

[43] Vincent I, Zheng JH, Dickson DW, Kress Y, Davies P. Mitotic phosphoepitopes precede paired helical filaments in Alzheimer's disease. Neurobiol Aging 1998;19. https://doi.org/10.1016/S0197-4580(98)00071-2.

[44] McKay GJ, Silvestri G, Chakravarthy U, Dasari S, Fritsche LG, Weber BH, et al. Variations in apolipoprotein e frequency with age in a pooled analysis of a large group of older people. Am J Epidemiol 2011;173. https://doi.org/10.1093/aje/kwr015.

[45] Yamazaki Y, Zhao N, Caulfield TR, Liu CC, Bu G. Apolipoprotein E and Alzheimer disease: pathobiology and targeting strategies. Nat Rev Neurol 2019;15. https://doi.org/10.1038/s41582-019-0228-7.

[46] Carter DB. The interaction of amyloid-beta with ApoE. Subcell Biochem 2005;38.

https://doi.org/10.1007/0-387-23226-5_13.

[47] Kanekiyo T, Bu G. The low-density lipoprotein receptor-related protein 1 and amyloid-β clearance in Alzheimer's disease. Front Aging Neurosci 2014;6. https://doi.org/10.3389/fnagi.2014.00093.

[48] Chen Y, Durakoglugil MS, Xian X, Herz J. ApoE4 reduces glutamate receptor function and synaptic plasticity by selectively impairing ApoE receptor recycling. Proc Natl Acad Sci U S A 2010;107. https://doi.org/10.1073/pnas.0914984107.

[49] Gilat-Frenkel M, Boehm-Cagan A, Liraz O, Xian X, Herz J, Michaelson D. Involvement of the Apoer2 and Lrp1 receptors in mediating the pathological effects of ApoE4 in vivo. Curr Alzheimer Res 2014;11. https://doi.org/10.2174/1567205010666131119232444.

[50] Wang L, Cooper JA. Optogenetic control of the Dab1 signaling pathway. Sci Rep 2017;7. https://doi.org/10.1038/srep43760.

[51] Hoe HS, Tran TS, Matsuoka Y, Howell BW, Rebeck GW. DAB1 and reelin effects on amyloid precursor protein and ApoE receptor 2 trafficking and processing. J Biol Chem 2006;281. https://doi.org/10.1074/jbc.M602162200.

[52] Dlugosz P, Nimpf J. The reelin receptors apolipoprotein e receptor 2 (ApoER2) and VLDL receptor. Int J Mol Sci 2018;19. https://doi.org/10.3390/ijms19103090.

[53] Holtzman DM, Herz J, Bu G. Apolipoprotein E and apolipoprotein E receptors: Normal biology and roles in Alzheimer disease. Cold Spring Harb Perspect Med 2012;2. https://doi.org/10.1101/cshperspect.a006312.

[54] Prume M, Rollenhagen A, Lübke JHR. Structural and Synaptic Organization of the Adult Reeler Mouse Somatosensory Neocortex: A Comparative Fine-Scale Electron Microscopic Study of Reeler With Wild Type Mice. Front Neuroanat 2018;12. https://doi.org/10.3389/fnana.2018.00080.

[55] Trommsdorff M, Gotthardt M, Hiesberger T, Shelton J, Stockinger W, Nimpf J, et al. Reeler/disabled-like disruption of neuronal migration in knockout mice lacking the VLDL receptor and ApoE receptor 2. Cell 1999;97. https://doi.org/10.1016/S0092-8674(00)80782-5.

[56] Hack I, Hellwig S, Junghans D, Brunne B, Bock HH, Zhao S, et al. Divergent roles of ApoER2 and Vldlr in the migration of cortical neurons. Development 2007;134. https://doi.org/10.1242/dev.005447.

[57] Callahan DG, Taylor WM, Tilearcio M, Cavanaugh T, Selkoe DJ, Young-Pearse TL. Embryonic mosaic deletion of APP results in displaced Reelin-expressing cells in the cerebral cortex. Dev Biol 2017;424. https://doi.org/10.1016/j.ydbio.2017.03.007.

[58] Chen Y, Beffert U, Ertunc M, Tang TS, Kavalali ET, Bezprozvanny I, et al. Reelin modulates NMDA receptor activity in cortical neurons. J Neurosci 2005;25. https://doi.org/10.1523/JNEUROSCI.1951-05.2005.

[59] Telese F, Ma Q, Perez PM, Notani D, Oh S, Li W, et al. LRP8-Reelin-Regulated Neuronal Enhancer Signature Underlying Learning and Memory Formation. Neuron 2015;86. https://doi.org/10.1016/j.neuron.2015.03.033.

[60] Hoe HS, Pocivavsek A, Chakraborty G, Fu Z, Vicini S, Ehlers MD, et al. Apolipoprotein E receptor 2 interactions with the N-Methyl-D-aspartate receptor. J Biol Chem 2006;281. https://doi.org/10.1074/jbc.M509380200.

[61] Beffert U, Weeber EJ, Durudas A, Qiu S, Masiulis I, Sweatt JD, et al. Modulation of synaptic plasticity and memory by Reelin involves differential splicing of the lipoprotein receptor Apoer2. Neuron 2005;47. https://doi.org/10.1016/j.neuron.2005.07.007.

[62] Pohlkamp T, Wasser CR, Herz J. Functional roles of the interaction of APP and

lipoprotein receptors. Front Mol Neurosci 2017;10. https://doi.org/10.3389/fnmol.2017.00054.

[63] Hoe H-S, Wessner D, Beffert U, Becker AG, Matsuoka Y, Rebeck GW. F-Spondin Interaction with the Apolipoprotein E Receptor ApoEr2 Affects Processing of Amyloid Precursor Protein. Mol Cell Biol 2005;25. https://doi.org/10.1128/mcb.25.21.9259-9268.2005.

[64] Müller T, Schrötter A, Loosse C, Pfeiffer K, Theiss C, Kauth M, et al. A ternary complex consisting of AICD, FE65, and TIP60 down-regulates Stathmin1. Biochim Biophys Acta - Proteins Proteomics 2013;1834. https://doi.org/10.1016/j.bbapap.2012.07.017.

[65] Hoe HS, Magill LA, Guenette S, Fu Z, Vicini S, Rebeck GW. FE65 interaction with the ApoE receptor ApoEr2. J Biol Chem 2006;281. https://doi.org/10.1074/jbc.M600728200.

[66] Main BF, Jones PJH, MacGillivray RTA, Banfield DK. Apolipoprotein E genotyping using the polymerase chain reaction and allele-specific oligonucleotide primers. J Lipid Res 1991;32. https://doi.org/10.1016/s0022-2275(20)42257-6.

[67] Medoro A, Bartollino S, Mignogna D, Marziliano N, Porcile C, Nizzari M, et al. Proteases Upregulation in Sporadic Alzheimer's Disease Brain. J Alzheimer's Dis 2019;68. https://doi.org/10.3233/JAD-181284.

[68] Kruse MN, Becker C, Lottaz D, Köhler D, Yiallouros I, Krell HW, et al. Human meprin α and β homo-oligomers: Cleavage of basement membrane proteins and sensitivity to metalloprotease inhibitors. Biochem J 2004;378. https://doi.org/10.1042/BJ20031163.

[69] Hampel H, Vassar R, De Strooper B, Hardy J, Willem M, Singh N, et al. The β-Secretase BACE1 in Alzheimer's Disease. Biol Psychiatry 2021;89.

https://doi.org/10.1016/j.biopsych.2020.02.001.

[70] Sun X, Tong Y, Qing H, Chen C-H, Song W. Increased BACE1 maturation contributes to the pathogenesis of Alzheimer's disease in Down syndrome. FASEB J 2006;20. https://doi.org/10.1096/fj.05-5628com.

[71] Neve RL, Boyce FM, McPhie DL, Greenan J, Oster-Granite M Lou. Transgenic mice expressing APP-C100 in the brain. Neurobiol Aging 1996;17. https://doi.org/10.1016/0197-4580(95)02074-8.